

## Supplementary information

### ***Diverse Reactivity of a Cationic N-Heterocyclic Phosphenium Complex towards Anionic Substrates – Substitution vs. Reduction***

Christoph M. Feil,<sup>a</sup> Florian Goerigk,<sup>a</sup> Yannick Stöckl,<sup>a</sup> Martin Nieger<sup>b</sup> and Dietrich Gudat<sup>\*a</sup>

<sup>a</sup> Institute of Inorganic Chemistry, University of Stuttgart, Stuttgart, Germany

<sup>b</sup> Department of Chemistry, University of Helsinki, University of Helsinki, Finland.

E-Mail: [dietrich.gudat@iac.uni-stuttgart.de](mailto:dietrich.gudat@iac.uni-stuttgart.de)

#### Table of contents

Table of contents	1
General conditions	2
Experimental Procedures	2
Crystallographic studies	5
EPR Spectra	9
NMR spectra	9
FTIR Spectra	27
Electrochemistry and Spectro-electrochemistry	31
Computational studies	33
References	35

## General conditions

Unless otherwise stated, all manipulations were carried out under an inert atmosphere of purified argon or nitrogen, either using flame-dried glassware and standard Schlenk techniques, or in gloveboxes. Benzene, Et<sub>2</sub>O, THF, and hexane were distilled from NaK alloy, toluene from Na, and CH<sub>2</sub>Cl<sub>2</sub> from CaH<sub>2</sub>, respectively, and stored in Schlenk-flasks under inert conditions. C<sub>6</sub>D<sub>6</sub> was refluxed over NaK alloy for 72 h, followed by distillation and storage over molecular sieves in a glovebox. Reaction monitoring experiments were carried out using NMR-tubes with a PTFE screw. [2]OTf,<sup>1</sup> **18b**,<sup>2</sup> **18c**,<sup>3</sup> [(benzylidene acetone)Fe(CO)<sub>3</sub>]<sup>4</sup> and bis(triphenylphosphine)iminium chloride<sup>5</sup> ([PPN]Cl) were prepared as described.

NMR spectra were acquired on Bruker Avance 250 (<sup>1</sup>H: 250.0 MHz, <sup>11</sup>B: 80.3 MHz, <sup>13</sup>C: 62.9 MHz, <sup>19</sup>F: 235.2 MHz, <sup>31</sup>P: 101.2 MHz) or Bruker Avance 400 (<sup>1</sup>H: 400.1 MHz, <sup>13</sup>C: 100.9 MHz, <sup>31</sup>P: 162.9 MHz) NMR spectrometers at 293 - 296 K if not stated otherwise. <sup>1</sup>H Chemical shifts were referenced to TMS using the signals of the residual protons of the deuterated solvent ( $\delta^1\text{H} = 7.15$  (C<sub>6</sub>D<sub>6</sub>), 7.27 (CDCl<sub>3</sub>), 1.73 (THF)) as secondary reference. Spectra of heteronuclei were referenced using the  $\Xi$ -scale<sup>6</sup> employing BF<sub>3</sub>·OEt<sub>2</sub> ( $\Xi = 32.083974$  MHz, <sup>11</sup>B), TMS ( $\Xi = 25.145020$  MHz, <sup>13</sup>C), CFC<sub>3</sub> ( $\Xi = 94.094011$  MHz, <sup>19</sup>F) and 85 % H<sub>3</sub>PO<sub>4</sub> ( $\Xi = 40.480747$  MHz, <sup>31</sup>P) as secondary references. Coupling constants are generally given as absolute values. Exchange broadened NMR signals (due to slow rotation of NDipp-groups) are denoted as "br". Assignments of <sup>1</sup>H, <sup>13</sup>C, and <sup>31</sup>P NMR signals of product mixtures were supported by <sup>1</sup>H,<sup>13</sup>C HSQC/HMBC and <sup>1</sup>H,<sup>31</sup>P HMQC NMR spectra. EPR spectra were recorded with a Magnetech MiniScope MS5000 spectrometer operating at a microwave frequency of 9.5 GHz (X-band) at room temperature. Spectral simulations were carried out with the Easyspin software.<sup>7</sup> FTIR spectra were recorded with a Thermo Scientific Nicolet iS5 spectrometer equipped with an iD5 attenuated total reflectance (ATR) unit under nitrogen atmosphere. Elemental analyses were performed with an Elementar Micro Cube elemental analyser.

## Experimental Procedures

**Synthesis of [3]OTf.** NHP salt [2]OTf<sup>1</sup> (0.56 g, 1.0 mmol) and Fe<sub>2</sub>(CO)<sub>9</sub> (0.36 g, 1.0 mmol) were suspended in Et<sub>2</sub>O (50 ml). The mixture was stirred for 20 h at rt. A yellow precipitate formed was collected by filtration, washed with Et<sub>2</sub>O (20 ml) and dried under reduced pressure. Yield 0.54 g (0.62 mmol, 62%). Single crystals suitable for XRD were obtained by recrystallisation from CH<sub>2</sub>Cl<sub>2</sub>/C<sub>6</sub>H<sub>6</sub> (1:1) at -24 °C.

<sup>1</sup>H NMR (CDCl<sub>3</sub>):  $\delta = 8.16$  (d, <sup>3</sup>J<sub>PH</sub> = 8.6 Hz, 2 H, NCH), 7.62 (m, 2 H, *p*-C<sub>6</sub>H<sub>3</sub>), 7.40 (m, 4 H, *m*-C<sub>6</sub>H<sub>3</sub>), 2.66 (sept, <sup>3</sup>J<sub>HH</sub> = 6.9 Hz, 4 H, CH), 1.33 (d, <sup>3</sup>J<sub>HH</sub> = 6.9 Hz, 12 H, CH<sub>3</sub>), 1.28 (d, <sup>3</sup>J<sub>HH</sub> = 6.9 Hz, 12 H, CH<sub>3</sub>). – <sup>31</sup>P{<sup>1</sup>H} NMR (CDCl<sub>3</sub>):  $\delta = 238.0$  (s). – <sup>19</sup>F NMR (CDCl<sub>3</sub>):  $\delta = -78.3$  (s). – <sup>13</sup>C{<sup>1</sup>H} NMR (CDCl<sub>3</sub>):  $\delta = 204.7$  (br s, CO), 146.1 (d, <sup>3</sup>J<sub>PC</sub> = 4.6 Hz, *o*-C), 134.8 (br s, NCH), 132.8 (br s, *p*-C), 129.3 (br s, *ipso*-C), 125.5 (br d, d, <sup>4</sup>J<sub>PC</sub> = 1.1 Hz, *m*-C), 29.4 (s, CH), 24.8 (s, CH<sub>3</sub>), 23.4 (s, CH<sub>3</sub>). The signal for the triflate anion was not detected. – FT-IR (pure solid):  $\tilde{\nu}$  [cm<sup>-1</sup>] = 2103 (s), 2037 (s), 2020 (s), 1948 (m)  $\nu$ CO. –C<sub>31</sub>H<sub>36</sub>F<sub>3</sub>FeN<sub>2</sub>O<sub>7</sub>PS (724.51 g mol<sup>-1</sup>): calcd. C 51.39 H 5.01 N 3.87, found C 50.93 H 5.01 N 4.01.

**Generation and characterisation of 6.** [3]OTf (45 mg, 62  $\mu$ mol) was dissolved in moist THF (5 ml). The resulting solution was stirred for 1 h and **6** identified in situ from the analysis of <sup>31</sup>P{<sup>1</sup>H} and <sup>1</sup>H,<sup>31</sup>P HMQC NMR spectra. Isolation of pure product was precluded by the occurrence of slow decomposition, but crystallization produced a few single crystals (no yield determined) one of which was identified as a 1:1 co-crystal of **6** and **7**, respectively.

Selected spectroscopic data: <sup>1</sup>H NMR (THF):  $\delta = 9.77$  (d, <sup>2</sup>J<sub>PH</sub> = 9.0 Hz, 1 H, POH), 6.21 (d, <sup>3</sup>J<sub>PH</sub> = 14.8 Hz, 2 H, NCH). – <sup>31</sup>P{<sup>1</sup>H} NMR (C<sub>6</sub>D<sub>6</sub>):  $\delta = 148.8$  (s).

**Synthesis of 8a.** [3]OTf (0.36 g, 0.50 mmol) and [Bu<sub>4</sub>N]F (0.14 g, 0.55 mmol) were suspended in toluene (8 ml). The mixture was stirred for 30 min. Volatiles were removed under reduced pressure, the residue taken up in hexane (15 ml) and the resulting suspension filtered. The filtrate was concentrated under reduced pressure to half of its original volume and stored at -24 °C for 24 h. The yellow crystals formed were collected by filtration and dried under reduced pressure. Yield 80 mg (0.14 mmol, 27%). The crystals were suitable for a XRD study.

<sup>1</sup>H NMR (C<sub>6</sub>D<sub>6</sub>):  $\delta = 7.28$ -6.99 (m, 6 H, C<sub>6</sub>H<sub>3</sub>), 5.93 (d, <sup>3</sup>J<sub>PH</sub> = 9.6 Hz, 2 H, NCH), 3.67 (sept, <sup>3</sup>J<sub>HH</sub> = 6.8 Hz, 2 H, CH), 3.19 (sept, <sup>3</sup>J<sub>HH</sub> = 6.8 Hz, 2 H, CH), 1.46-1.30 (m, 12 H, CH<sub>3</sub>), 1.17-1.04 (m, 12 H, CH<sub>3</sub>). – <sup>31</sup>P{<sup>1</sup>H} NMR (C<sub>6</sub>D<sub>6</sub>):  $\delta = 161.5$  (d, <sup>1</sup>J<sub>PF</sub> = 1175 Hz). – <sup>31</sup>P NMR (C<sub>6</sub>D<sub>6</sub>)  $\delta = 161.5$  (dt, <sup>1</sup>J<sub>PF</sub> = 1175 Hz, <sup>3</sup>J<sub>PH</sub> = 9.6 Hz). – <sup>19</sup>F NMR (C<sub>6</sub>D<sub>6</sub>):  $\delta = 30.1$  (d, <sup>1</sup>J<sub>PF</sub> = 1175 Hz). – <sup>13</sup>C{<sup>1</sup>H} NMR (C<sub>6</sub>D<sub>6</sub>)  $\delta = 211.9$  (dd, <sup>2</sup>J<sub>PC</sub> = 14.5 Hz, <sup>3</sup>J<sub>FC</sub> = 3.8 Hz, CO), 148.4 (m, *o*-C), 147.5 (m, *o*-C), 132.9 (dd, <sup>2</sup>J<sub>PC</sub> = 8.3 Hz, <sup>3</sup>J<sub>FC</sub> = 1.2 Hz, *ipso*-C), 128.9 (d, <sup>5</sup>J<sub>PC</sub> = 1.8 Hz, *p*-C), 124.0 (br s, *m*-C), 123.3 (br s, *m*-C), 118.8 (d, <sup>3</sup>J<sub>PC</sub> = 3.5 Hz, NCH), 28.0 (s, CH), 27.4 (d, <sup>4</sup>J<sub>PC</sub> = 3.7 Hz, CH), 25.8 (s, CH<sub>3</sub>), 24.3 (s, CH<sub>3</sub>), 22.7 (s, CH<sub>3</sub>), 21.7 (s, CH<sub>3</sub>). – FTIR (pure

solid):  $\tilde{\nu}$  [cm<sup>-1</sup>] = 2072 (m), 1988 (s), 1949 (s),  $\nu$ CO. – C<sub>30</sub>H<sub>36</sub>FFeN<sub>2</sub>O<sub>4</sub>P (594.45 g mol<sup>-1</sup>): calcd. C 60.62 H 6.10 N 4.71, found C 60.74 H 6.55 N 4.74.

**Synthesis of 8b.** [3]OTf and [PPN]Cl<sup>5</sup> were suspended in benzene (10 ml). The mixture was stirred for 2 h at rt. Volatiles were removed under reduced pressure, the residue taken up in hexane (20 ml) and the resulting suspension filtered. The filtrate was concentrated under reduced pressure to half of its original volume and stored at -24 °C for 24 h. The brownish yellow crystals formed were collected by filtration and dried under reduced pressure. Yield 50 mg (80  $\mu$ mol, 17%). The crystals were suitable for a XRD study.

<sup>1</sup>H NMR (C<sub>6</sub>D<sub>6</sub>):  $\delta$  = 7.26–6.96 (m, 6 H, C<sub>6</sub>H<sub>3</sub>), 6.00 (d, <sup>3</sup>J<sub>PH</sub> = 6.7 Hz, 2 H, NCH), 4.09 (br, 2 H, CH), 3.15 (br, 2 H, CH), 1.40 (br d, <sup>3</sup>J<sub>HH</sub> = 6.6 Hz, 12 H, CH<sub>3</sub>), 1.09 (br m, 12 H, CH<sub>3</sub>). – <sup>31</sup>P{<sup>1</sup>H} NMR (C<sub>6</sub>D<sub>6</sub>):  $\delta$  = 166.4 (s). – <sup>13</sup>C{<sup>1</sup>H} NMR (C<sub>6</sub>D<sub>6</sub>):  $\delta$  = 213.2 (d, <sup>2</sup>J<sub>PC</sub> = 6.2 Hz, CO), 149.5 (br, *o*-C), 148.3 (br, *o*-C), 133.8 (d, <sup>2</sup>J<sub>PC</sub> = 8.3 Hz, *ipso*-C), 130.0 (d, <sup>5</sup>J<sub>PC</sub> = 2.3 Hz, *p*-C), 125.5 (br, *m*-C), 124.1 (br, *m*-C), 121.5 (br, NCH), 29.0 (br, CH), 26.5 (br, CH<sub>3</sub>), 25.4 (s, CH<sub>3</sub>), 24.4 (s, CH<sub>3</sub>), 22.2 (s, CH<sub>3</sub>). – FTIR (solid):  $\tilde{\nu}$  [cm<sup>-1</sup>] = 2072 (m), 1987 (s), 1957 (s),  $\nu$ CO. – C<sub>30</sub>H<sub>36</sub>ClFeN<sub>2</sub>O<sub>4</sub>P (594.45 g mol<sup>-1</sup>): calcd. C 58.98 H 5.94 N 4.59, found C 58.90 H 6.11 N 4.60.

**Synthesis of 9.** Li[HBET<sub>3</sub>] (0.64 ml of a 1 M Lösung in THF, 0.64 mmol) was added to a stirred solution of [3]OTf (0.46 g, 0.64 mmol) in toluene (10 ml) at rt. While stirring was continued for 10 min, the colour of the mixture changed from yellow to brown. Volatiles were removed under reduced pressure, the residue treated with hexane (20 ml) and the resulting suspension filtered. The filtrate was concentrated under reduced pressure to half of its volume and stored at -24 °C for 24 h. Yellow crystals formed were collected by filtration and dried under reduced pressure. Yield 0.11 g (0.19 mmol, 30%).

<sup>1</sup>H NMR (C<sub>6</sub>D<sub>6</sub>):  $\delta$  = 9.75 (d, <sup>1</sup>J<sub>PH</sub> = 349 Hz, 1 H, PH), 7.25–7.00 (m, 6 H, C<sub>6</sub>H<sub>3</sub>), 5.84 (d, <sup>3</sup>J<sub>PH</sub> = 12.0 Hz, 2 H, NCH), 3.72 (sept, <sup>3</sup>J<sub>HH</sub> = 6.9 Hz, 2 H, CH), 3.30 (sept, <sup>3</sup>J<sub>HH</sub> = 6.8 Hz, 2 H, CH), 1.46 (d, <sup>3</sup>J<sub>HH</sub> = 6.9 Hz, 6 H, CH<sub>3</sub>), 1.29 (d, <sup>3</sup>J<sub>HH</sub> = 6.9 Hz, 6 H, CH<sub>3</sub>), 1.16 (d, <sup>3</sup>J<sub>HH</sub> = 6.8 Hz, 12 H, CH<sub>3</sub>). – <sup>31</sup>P{<sup>1</sup>H} NMR (C<sub>6</sub>D<sub>6</sub>):  $\delta$  [ppm]: 137.6 (s). – <sup>31</sup>P NMR (C<sub>6</sub>D<sub>6</sub>):  $\delta$  = 137.6 (dt, <sup>1</sup>J<sub>PH</sub> = 349 Hz, <sup>3</sup>J<sub>PH</sub> = 12.0 Hz). – <sup>13</sup>C{<sup>1</sup>H} NMR (C<sub>6</sub>D<sub>6</sub>):  $\delta$  = 211.8 (d, <sup>2</sup>J<sub>PC</sub> = 18.5 Hz, CO), 149.4 (d, <sup>3</sup>J<sub>PC</sub> = 3.3 Hz, *o*-C), 148.9 (d, <sup>3</sup>J<sub>PC</sub> = 1.5 Hz, *o*-C), 133.9 (d, <sup>2</sup>J<sub>PC</sub> = 4.5 Hz, *ipso*-C), 129.3 (d, <sup>5</sup>J<sub>PC</sub> = 1.5 Hz, *p*-C), 124.7 (br s, *m*-C), 124.4 (d, <sup>4</sup>J<sub>PC</sub> = 1.4 Hz, *m*-C), 121.7 (d, <sup>2</sup>J<sub>PC</sub> = 4.5 Hz, NCH), 29.5 (s, CH), 28.4 (s, CH), 26.2 (s, CH<sub>3</sub>), 24.6 (s, CH<sub>3</sub>), 22.9 (s, CH<sub>3</sub>), 22.7 (s, CH<sub>3</sub>). – FTIR (pur solid):  $\tilde{\nu}$  = 2185 (w,  $\nu$ PH), 2049 (m), 2022 (m), 1936 (s) (all  $\nu$ CO) cm<sup>-1</sup>. – C<sub>30</sub>H<sub>37</sub>FeN<sub>2</sub>O<sub>4</sub>P (576.45 g mol<sup>-1</sup>): calcd. C 62.51 H 6.47 N 4.86, found C 62.51 H 6.51 N 4.77.

**Synthesis of 10c. Method A:** A suspension of [3]OTf (362 mg, 500  $\mu$ mol) and KBr (66 mg, 550  $\mu$ mol) in toluene (5 ml) was stirred for 20 h at rt. The solvent was removed under reduced pressure, the residue taken up in Et<sub>2</sub>O (20 ml) and the resulting suspension filtered. The volume of the filtrate was reduced to 10 ml and hexane (30 ml) added. Storage of the solution at -24 °C for 24 h produced deep red crystals, which were collected by filtration and dried under reduced pressure. Yield 78 mg (0.13 mmol, 25%). The crystals were suitable for a XRD study.

**Method B:** A solution of **17c** (400 mg, 820  $\mu$ mol) and Fe<sub>2</sub>(CO)<sub>9</sub> (370 mg, 1.02 mmol) in toluene (10 ml) was stirred for 30 min at rt. Volatiles were removed under reduced pressure and the residue dissolved in Et<sub>2</sub>O (20 ml). The resulting solution was concentrated to half its original volume under reduced pressure and the product precipitated by addition of hexane (30 ml). The deep red solid formed was collected by filtration and dried under reduced pressure. Yield 280 mg (450  $\mu$ mol, 56%).

<sup>1</sup>H NMR (C<sub>6</sub>D<sub>6</sub>):  $\delta$  = 7.24–6.99 (m, 6 H, C<sub>6</sub>H<sub>3</sub>), 6.09 (d, <sup>3</sup>J<sub>PH</sub> = 5.2 Hz, 2 H, NCH), 3.00 (sept, <sup>3</sup>J<sub>HH</sub> = 6.8 Hz, 4 H, CH), 1.36 (d, <sup>3</sup>J<sub>HH</sub> = 6.8 Hz, 12 H, CH<sub>3</sub>), 1.05 (d, <sup>3</sup>J<sub>HH</sub> = 6.8 Hz, 12 H, CH<sub>3</sub>). – <sup>31</sup>P{<sup>1</sup>H} NMR (C<sub>6</sub>D<sub>6</sub>):  $\delta$  = 218.1 (s). – <sup>13</sup>C{<sup>1</sup>H} NMR (C<sub>6</sub>D<sub>6</sub>):  $\delta$  = 146.7 (d, <sup>3</sup>J<sub>PC</sub> = 2.7 Hz, *o*-C), 132.2 (d, <sup>2</sup>J<sub>PC</sub> = 6.2 Hz, *ipso*-C), 130.9 (s, *p*-C), 124.7 (s, *m*-C), 124.1 (d, <sup>2</sup>J<sub>PC</sub> = 2.8 Hz, NCH), 29.1 (s, CH), 24.7 (s, CH<sub>3</sub>), 23.3 (s, CH<sub>3</sub>). The signal of the CO ligands was not detectable because of the low S/N ratio. – FTIR (pure solid):  $\tilde{\nu}$  [cm<sup>-1</sup>] = 2046 (m), 1989 (s), 1959 (s),  $\nu$ CO. – C<sub>29</sub>H<sub>36</sub>BrFeN<sub>2</sub>O<sub>3</sub>P (627.34 g mol<sup>-1</sup>): calcd. C 55.52 H 5.78 N 4.47, found C 52.10 H 6.04 N 4.37.

**Synthesis of 10d.** A suspension of [3]OTf (1.45 g, 2.00 mmol) and KI (360 mg, 2.20 mmol) in toluene was stirred for 48 h at rt. The solvent was removed under reduced pressure, the residue taken up in Et<sub>2</sub>O (50 ml) and the resulting suspension filtered. The volume of the filtrate was reduced to 20 ml and hexane (60 ml) added. Storage of the solution at -24 °C for 24 h produced deep red crystals, which were collected by filtration and dried under reduced pressure. Yield 420 mg (630  $\mu$ mol, 32%). The crystals were suitable for a XRD study.

<sup>1</sup>H NMR (CDCl<sub>3</sub>):  $\delta$  = 7.55–7.44 (m, 2 H, *p*-C<sub>6</sub>H<sub>3</sub>), 7.33 (m, 4 H, *m*-C<sub>6</sub>H<sub>3</sub>), 6.78 (d, <sup>3</sup>J<sub>PH</sub> = 6.0 Hz, 2 H, NCH), 2.97 (sept, <sup>3</sup>J<sub>HH</sub> = 6.8 Hz, 4 H, CH), 1.35 (d, <sup>3</sup>J<sub>HH</sub> = 6.8 Hz, 12 H, CH<sub>3</sub>), 1.25 (d, <sup>3</sup>J<sub>HH</sub> = 6.8 Hz, 12 H, CH<sub>3</sub>). – <sup>31</sup>P{<sup>1</sup>H} NMR (CDCl<sub>3</sub>):  $\delta$  = 220.0 (s). – <sup>13</sup>C{<sup>1</sup>H} NMR (CDCl<sub>3</sub>):  $\delta$  = 214.5 (br s, CO), 147.0 (br s, *o*-C), 132.0 (d, <sup>2</sup>J<sub>PC</sub> = 7.0 Hz, *ipso*-C), 130.9 (br s, *p*-C), 125.1 (br s, *m*-C), 124.8 (br s, NCH), 29.3 (s, CH), 25.1 (s, CH<sub>3</sub>), 23.6 (s, CH<sub>3</sub>). – FTIR (pure solid):  $\tilde{\nu}$  [cm<sup>-1</sup>] = 2046

(m), 1994 (s), 1969 (s),  $\nu\text{CO}$ . –  $\text{C}_{29}\text{H}_{36}\text{FeIN}_2\text{O}_3\text{P}$  (674.34 g mol<sup>-1</sup>): calcd. C 51.65 H 5.38 N 4.15, found C 51.24 H 5.21 N 4.08.

**Reaction of [3]OTf with LDA.** LDA (275  $\mu\text{L}$  of a 2.0 M solution in THF, 550  $\mu\text{mol}$ ) was added to a stirred solution of [3]OTf (362 mg, 500  $\mu\text{mol}$ ) in THF (3-5 ml) and the progress of the reaction analysed by NMR (Figure S4) and EPR spectroscopy (Figure S4). Similar experiments were carried out using *t*BuLi and MHMDS (M = Li, K; HMDS = hexamethyldisilazane), or under addition of LDA at -78 °C (see Figure S4).

**Synthesis of [15]OTf.** A suspension of [3]OTf (724 mg, 1.00 mmol) and  $\text{PPh}_3$  (288 mg, 1.10 mmol) in toluene (15 ml) was stirred at 80 °C for 20 h. The mixture was allowed to cool to rt, the yellow-orange precipitate collected by filtration, washed with hexane (20 ml) and dried under reduced pressure. Yield 740 mg (750  $\mu\text{mol}$ , 75%).

<sup>1</sup>H NMR ( $\text{CDCl}_3$ ):  $\delta$  = 7.58 (d, <sup>3</sup>*J*<sub>PH</sub> = 8.6 Hz, 2H, NCH), 7.55-7.00 (m, 21 H, C<sub>6</sub>H<sub>3</sub> and C<sub>6</sub>H<sub>5</sub>), 2.86 (sept, <sup>3</sup>*J*<sub>HH</sub> = 6.8 Hz, 4 H, CH), 1.27 (d, <sup>3</sup>*J*<sub>HH</sub> = 6.8 Hz, 12 H, CH<sub>3</sub>), 1.19 (d, <sup>3</sup>*J*<sub>HH</sub> = 6.8 Hz, 12 H, CH<sub>3</sub>). – <sup>31</sup>P{<sup>1</sup>H} NMR ( $\text{CDCl}_3$ ):  $\delta$  = 242.3 (d, <sup>2</sup>*J*<sub>PP</sub> = 47 Hz, P<sup>NHP</sup>), 53.2 (d, <sup>2</sup>*J*<sub>PP</sub> = 47 Hz, PPh<sub>3</sub>). – <sup>19</sup>F NMR ( $\text{CDCl}_3$ ):  $\delta$  = -78.2 (s). – <sup>13</sup>C{<sup>1</sup>H} NMR ( $\text{CDCl}_3$ ):  $\delta$  = 210.9 (dd, <sup>2</sup>*J*<sub>PC</sub> = 15.1 Hz, 21.6 Hz, CO), 146.2 (d, <sup>3</sup>*J*<sub>PC</sub> = 4.0 Hz, *o*-C), 132.9 (d, <sup>2</sup>*J*<sub>PC</sub> = 11.1 Hz, *o*-C), 131.8 (m, *ipso*-C), 131.4 (s, NCH), 131.0 (m, *p*-C, *ipso*-C), 129.1 (d, <sup>3</sup>*J*<sub>PC</sub> = 11.1 Hz, *m*-C), 125.0 (s, *m*-C), 29.5 (s, CH), 25.6 (s, CH<sub>3</sub>), 22.8 (s, CH<sub>3</sub>). The signal of the anion was not detected. – FTIR (pure solid):  $\tilde{\nu}$  [cm<sup>-1</sup>] = 2053 (m), 1989 (br, s),  $\nu\text{CO}$ . –  $\text{C}_{48}\text{H}_{51}\text{F}_3\text{FeN}_2\text{O}_6\text{P}_2\text{S}$  (958.79 g mol<sup>-1</sup>): calcd. C 60.13 H 5.36 N 2.92, found C 59.81 H 5.35 N 3.07.

**Generation and characterization of 16.** A solution of [15]OTf (100 mg, 100  $\mu\text{mol}$ ) in THF (3 ml) was cooled to -78 °C. A solution of LDA (12 mg, 0.11 mmol) in THF (2 ml) was added dropwise and the resulting mixture stirred for 10 min.  $\text{BEt}_3$  (120  $\mu\text{l}$  of a 1 M solution in THF, 0.12 mmol) was added, the mixture allowed to warm slowly to rt and stirred for additional 30 min. The mixture was filtered through a bed of silica and the solvent removed under reduced pressure. The residue was treated with hexane (5 ml) and the resulting suspension filtered. Storage of the filtrate at -24 °C for 24 h produced an orange-red, inhomogeneous precipitate that was collected by filtration and dried under reduced pressure. Spectroscopic analysis revealed the presence of a mixture containing **16** (approx. 85% by NMR, identified by its spectroscopic data),  $[\text{Fe}(\text{CO})_3(\text{PPh}_3)_2]^8$  (approx. 8-10%, formed during work-up), and traces of  $\text{PPh}_3$  and additional unidentified side products that could not be further separated. A crystal of **16** suitable for an XRD study was obtained by manual selection. No yield determined. Elemental analysis: C 70.13 H 7.42 N 2.85 (cf. C 70.21 H 7.23 N 3.09 calcd. for  $\text{C}_{53}\text{H}_{65}\text{BFeN}_2\text{O}_3\text{P}_2$  (906.72 g mol<sup>-1</sup>, **16**)).

Spectroscopic data for **16**: <sup>1</sup>H NMR ( $\text{C}_6\text{D}_6$ ):  $\delta$  = 7.83 (d, <sup>3</sup>*J*<sub>PH</sub> = 5.7 Hz, 1 H, NCH), 3.15 (sept, <sup>3</sup>*J*<sub>HH</sub> = 6.7 Hz, 2 H, CH), 3.06 (sept, <sup>3</sup>*J*<sub>HH</sub> = 6.8 Hz, 2 H, CH), 1.60 (d, <sup>3</sup>*J*<sub>HH</sub> = 6.7 Hz, 6 H, CH<sub>3</sub>), 1.48 (d, <sup>3</sup>*J*<sub>HH</sub> = 6.8 Hz, 6 H, CH<sub>3</sub>), 1.35 (m, 15 H, CH<sub>3</sub> and  $\text{BCCH}_3$ ), 1.23 (d, <sup>3</sup>*J*<sub>HH</sub> = 6.7 Hz, 6 H, CH<sub>3</sub>), 0.83 (q, <sup>3</sup>*J*<sub>HH</sub> = 7.5 Hz, 6 H,  $\text{BCH}_2$ ); signals at 7.82-6.80 arise from the overlay of the signals of the C<sub>6</sub>H<sub>3</sub>-unit in **17** and the C<sub>6</sub>H<sub>5</sub> moieties in all components present and are not assignable in detail. – <sup>31</sup>P{<sup>1</sup>H} NMR ( $\text{C}_6\text{D}_6$ ):  $\delta$  = 258.1 (d, <sup>2</sup>*J*<sub>PP</sub> = 72 Hz, P<sup>NHP</sup>), 79.4 (d, <sup>2</sup>*J*<sub>PP</sub> = 72 Hz, PPh<sub>3</sub>). – <sup>11</sup>B{<sup>1</sup>H} NMR ( $\text{C}_6\text{D}_6$ ):  $\delta$  = -7.4 (s). – FTIR (solid):  $\tilde{\nu}$  [cm<sup>-1</sup>] = 1929 (s), 1890 (br, s),  $\nu\text{CO}$ .

Spectroscopic data for  $[\text{Fe}(\text{CO})_3(\text{PPh}_3)_2]$ : <sup>31</sup>P{<sup>1</sup>H} NMR ( $\text{C}_6\text{D}_6$ ):  $\delta$  = 82.9 (s). – FTIR (solid):  $\tilde{\nu}$  [cm<sup>-1</sup>] = 1885, 1873,  $\nu\text{CO}$ .

**Synthesis of (12)<sub>2</sub>.** A solution of **17b**<sup>2</sup> (500 mg, 1.13 mmol) and  $[(\text{ba})\text{Fe}(\text{CO})_3]^4$  (484 mg, 1.69 mmol) in toluene (4 ml) was stirred for 2 h at 50 °C. The mixture was allowed to cool to rt and the selective formation of (12)<sub>2</sub> verified by NMR spectroscopy. Volatiles were then removed under reduced pressure, the residue treated with hexane (60 ml), and the resulting mixture filtered. Storage of the filtrate at -24 °C for 48 h gave a small yield of deep red crystals that were suitable for XRD studies. Yield 22 mg, 20  $\mu\text{mol}$ , 4%.

<sup>1</sup>H NMR ( $\text{C}_6\text{D}_6$ ):  $\delta$  = 7.26-7.05 (m, 12 H, C<sub>6</sub>H<sub>3</sub>), 6.14 (d, <sup>3</sup>*J*<sub>PH</sub> = 4.4 Hz, 4 H, NCH), 3.32 (sept, <sup>3</sup>*J*<sub>HH</sub> = 6.8 Hz, 8 H, CH), 1.38 (d, <sup>3</sup>*J*<sub>HH</sub> = 6.8 Hz, 24 H, CH<sub>3</sub>), 1.11 (d, <sup>3</sup>*J*<sub>HH</sub> = 6.8 Hz, 24 H, CH<sub>3</sub>). – <sup>31</sup>P{<sup>1</sup>H} NMR ( $\text{C}_6\text{D}_6$ ):  $\delta$  = 239.1 (s). – <sup>13</sup>C{<sup>1</sup>H} NMR ( $\text{C}_6\text{D}_6$ ):  $\delta$  = 221.6 (s, CO), 148.4 (m, *o*-C), 134.0 (m, *ipso*-C), 129.7 (s, *p*-C), 124.4 (s, NCH), 124.1 (s, *m*-C), 28.8 (s, CH), 25.2 (s, CH<sub>3</sub>), 23.0 (s, CH<sub>3</sub>). – FTIR (pure solid):  $\tilde{\nu}$  = 1997 (m), 1948 (m), 1920 (s) cm<sup>-1</sup>,  $\nu\text{CO}$ . –  $\text{C}_{58}\text{H}_{72}\text{Fe}_2\text{N}_4\text{O}_6\text{P}_2$  (1094.87 g mol<sup>-1</sup>): calcd. C 63.63 H 6.63 N 5.12, found C 61.28 H 6.67 N 4.96.

## Crystallographic studies

Single-crystal X-ray diffraction data were measured on a Bruker Kappa APEX2 Duo diffractometer at 130(2) K or 135(2) K using Mo- $K_{\alpha}$  radiation ( $\lambda = 0.71073 \text{ \AA}$ ) or Cu- $K_{\alpha}$  radiation ( $\lambda = 1.54178 \text{ \AA}$ ), respectively. The structures were solved by Direct methods (SHELXS<sup>9</sup>) or dual space / intrinsic methods (SHELXT<sup>10</sup>), and refined with a full-matrix-least-squares scheme on  $F^2$  (SHELXL<sup>11</sup>). Semi-empirical or numerical absorption corrections were applied. Non-hydrogen atoms were refined anisotropically. Hydrogen atoms bound to O and P atoms were refined freely and all others using a riding model. For **8b**, the absolute structure was determined crystallographically by refinement of Parsons' Flack parameter  $x$ .<sup>12</sup> The P(H)(=O) moiety of **7** in the co-crystal of {**6-7**} and the P(H)Fe(CO)<sub>4</sub> moiety in **9** are disordered (see cif-files for details).

CCDC 2394830 - 2394839 contain the supplementary crystallographic data for this paper. These data can be obtained free of charge from The Cambridge Crystallographic Data Centre via [www.ccdc.cam.ac.uk/data\\_request/cif](http://www.ccdc.cam.ac.uk/data_request/cif).

**Table S1.** X-Ray Diffraction Details for [3]OTf, {6-7}, **8a**, **8b**, **9**, **10c**, **10d**, (**12**)<sub>2</sub> and **16**.

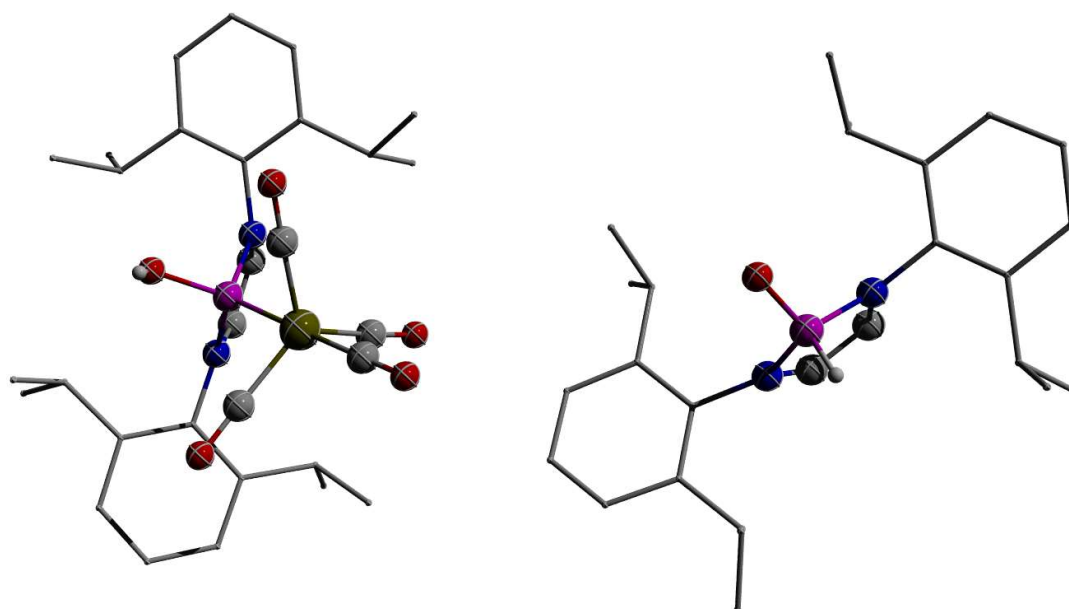
	[3]OTf	{6-7}	8a
Empirical formula	C <sub>30</sub> H <sub>36</sub> FeN <sub>2</sub> O <sub>4</sub> P · CF <sub>3</sub> O <sub>3</sub> S	C <sub>30</sub> H <sub>37</sub> FeN <sub>2</sub> O <sub>5</sub> P C <sub>26</sub> H <sub>37</sub> N <sub>2</sub> OP	C <sub>30</sub> H <sub>36</sub> FFeN <sub>2</sub> O <sub>4</sub> P
Formula weight (g·mol <sup>-1</sup> )	724.50	1016.98	594.43
<i>T</i> (K)	130(2)	135(2)	135(2)
Crystal size (mm)	0.22 × 0.14 × 0.11	0.24 × 0.18 × 0.10	0.23 × 0.20 × 0.18
Wavelength (Å)	0.71073	0.71073	0.71073
Space group	<i>P2</i> <sub>1</sub> / <i>n</i>	<i>P2</i> <sub>1</sub> / <i>n</i>	<i>P2</i> <sub>1</sub> / <i>c</i>
<i>a</i> (Å)	10.6034(4)	19.0542(7)	9.3489(2)
<i>b</i> (Å)	14.1577(5)	12.7479(5)	15.7776(4)
<i>c</i> (Å)	24.0619(8)	22.9643(9)	20.7100(5)
$\alpha$ (deg)	90	90	90
$\beta$ (deg)	98.392(1)	96.523(1)	94.160(1)
$\gamma$ (deg)	90	90	90
<i>V</i> (Å <sup>3</sup> )	3573.5(2)	5541.9(4)	3046.74(13)
<i>Z</i>	4	4	4
<i>D</i> <sub>c</sub> (mg·m <sup>-3</sup> )	1.347	1.219	1.296
$\mu$ (mm <sup>-1</sup> )	0.59	0.38	0.59
<i>F</i> (000)	1504	2168	1248
$\theta$ -range (deg)	1.7 to 28.3	1.5 to 26.4	1.6 to 26.4
Reflections collected	35481	46095	28961
Unique reflections	8839	11313	6229
Unique reflections with $I > 2\sigma(I)$	6413	8331	5169
<i>R</i> <sub>int</sub>	0.041	0.047	0.024
max./min transmission	0.746/0.700	0.745/0.662	0.745/0.699
Absorption correction	multi-scan	multi-scan	multi-scan
Data/restraints/parameters	8839/0/415	11313/70/649	6229/0/352
G.o.F. on $F^2$	1.01	1.02	1.03
<i>R</i> 1 [ $I > 2\sigma(I)$ ]	0.039	0.045	0.034
<i>wR</i> 2 ( $F^2$ ) (all data)	0.091	0.108	0.091
Largest diff. peak/hole (eÅ <sup>-3</sup> )	0.43/-0.35	0.36/-0.71	1.30/-0.29
Absolute structure parameter			
CCDC	2394831	2394836	2394834

Table S1 (continued).

	8b	9	10c
Empirical formula	C <sub>30</sub> H <sub>36</sub> ClFeN <sub>2</sub> O <sub>4</sub> P	C <sub>30</sub> H <sub>37</sub> FeN <sub>2</sub> O <sub>4</sub> P	C <sub>29</sub> H <sub>36</sub> BrFeN <sub>2</sub> O <sub>3</sub> P
Formula weight (g·mol <sup>-1</sup> )	610.88	576.43	627.33
T (K)	135(2)	135(2)	135(2)
Crystal size (mm)	0.39 × 0.16 × 0.14	0.44 × 0.30 × 0.16	0.16 × 0.11 × 0.05
Wavelength (Å)	0.71073	0.71073	0.71073
Space group	<i>P2<sub>1</sub>2<sub>1</sub>2<sub>1</sub></i>	<i>Pnma</i>	<i>P2<sub>1</sub>/n</i>
a (Å)	9.3014(4)	19.504(3)	10.4231(5)
b (Å)	15.9429(6)	20.268(3)	15.9589(7)
c (Å)	20.7089(9)	7.7710(11)	18.5439(8)
α (deg)	90	90	90
β (deg)	90	90	97.918(2)
γ (deg)	90	90	90
V (Å <sup>3</sup> )	3070.9(2)	3071.9(7)	3055.2(2)
Z	4	4	4
D <sub>c</sub> (mg·m <sup>-3</sup> )	1.321	1.246	1.364
μ (mm <sup>-1</sup> )	0.67	0.58	1.88
F(000)	1280	1216	1296
θ-range (deg)	1.6 to 33.2	2.1 to 26.4	1.7 to 26.4
Reflections collected	61876	20806	26328
Unique reflections	11742	3136	6220
Unique reflections with I > 2σ (I)	10637	2023	4592
R <sub>int</sub>	0.028	0.077	0.041
max./min transmission	0.747/0.696	0.986/0.547	0.958/0.787
Absorption correction	multi-scan	numerical	numerical
Data/restraints/parameters	11742/0/352	3136/268/240	6220/0/334
G.o.F. on F <sup>2</sup>	1.03	1.12	1.01
R1 [I > 2σ(I)]	0.027	0.108	0.034
wR2 (F <sup>2</sup> ) (all data)	0.066	0.321	0.077
Largest diff. peak/hole (eÅ <sup>-3</sup> )	0.44/-0.22	1.82/-0.64	0.42/-0.25
Absolute structure parameter	0.000(3)		
CCDC	2394838	2394833	2394835

**Table S1** (continued).

	<b>10d</b>	<b>(12)<sub>2</sub></b>	<b>16</b>
Empirical formula	C <sub>29</sub> H <sub>36</sub> FeIN <sub>2</sub> O <sub>3</sub> P	C <sub>58</sub> H <sub>72</sub> Fe <sub>2</sub> N <sub>4</sub> O <sub>6</sub> P <sub>2</sub> · C <sub>6</sub> H <sub>14</sub>	C <sub>53</sub> H <sub>65</sub> BFeN <sub>2</sub> O <sub>3</sub> P <sub>2</sub> · 0.5(C <sub>6</sub> H <sub>14</sub> )
Formula weight (g·mol <sup>-1</sup> )	674.32	1181.00	949.75
<i>T</i> (K)	135(2)	130(2)	135(2)
Crystal size (mm)	0.09 × 0.08 × 0.06	0.59 × 0.35 × 0.24	0.10 × 0.07 × 0.04
Wavelength (Å)	1.54178	0.71073	1.54178
Space group	<i>P</i> 2 <sub>1</sub> / <i>c</i>	<i>P</i> 2 <sub>1</sub> / <i>c</i>	<i>P</i> 1
<i>a</i> (Å)	10.5577(4)	17.1451(16)	11.7867(8)
<i>b</i> (Å)	15.8428(6)	17.4275(14)	14.0597(8)
<i>c</i> (Å)	18.8333(6)	21.318(2)	16.5324(10)
$\alpha$ (deg)	90	90	91.523(5)
$\beta$ (deg)	99.915(2)	92.412(4)	97.740(4)
$\gamma$ (deg)	90	90	104.937(5)
<i>V</i> (Å <sup>3</sup> )	3103.07(19)	6364.2(10)	2617.6(3)
<i>Z</i>	4	4	2
<i>D<sub>c</sub></i> (mg·m <sup>-3</sup> )	1.443	1.233	1.205
$\mu$ (mm <sup>-1</sup> )	12.44	0.56	3.22
<i>F</i> (000)	1368	2512	1014
$\theta$ -range (deg)	3.7 to 66.6	1.5 to 28.3	2.7 to 66.6
Reflections collected	19055	64255	33473
Unique reflections	5295	15624	8928
Unique reflections with <i>I</i> > 2 $\sigma$ ( <i>I</i> )	4412	12115	5336
<i>R</i> <sub>int</sub>	0.055	0.031	0.124
max./min transmission	0.699/0.560	0.746/0.657	0.749/0.647
Absorption correction	numerical	multi-scan	multi-scan
Data/restraints/parameters	5295/0/334	15624/0/703	8928/0/586
G.o.F. on <i>F</i> <sup>2</sup>	1.03	1.01	1.01
<i>R</i> 1 [ <i>I</i> > 2 $\sigma$ ( <i>I</i> )]	0.032	0.036	0.055
<i>wR</i> 2 ( <i>F</i> <sup>2</sup> ) (all data)	0.074	0.090	0.133
Largest diff. peak/hole (eÅ <sup>-3</sup> )	0.45/-0.39	0.46/-0.33	0.37/-0.36
CCDC	2394832	2394830	2394839



**Figure S1.** Representation of the molecular structures of **6** (left) and **7** (right) in the 1:1 co-crystal. Only one of the disordered P(H)O-units of **7** is displayed. For clarity, hydrogen atoms were omitted and the N-Dipp units drawn using a wire model. Thermal ellipsoids were drawn at the 50% probability level.

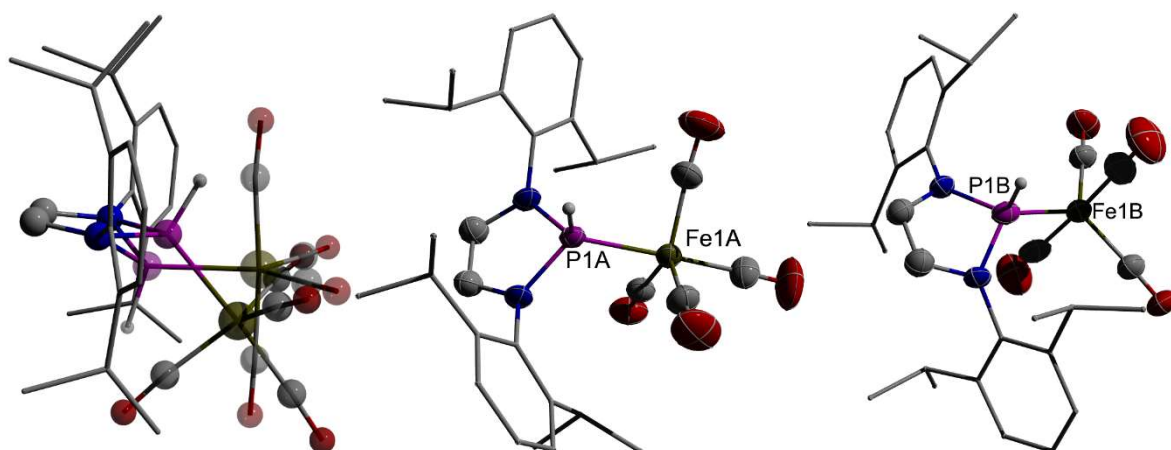


**Figure S2.** Representation of the disordered molecular structure of **9** in the crystal and the separated structures of the stereoisomers **9<sub>ax</sub>** (occupancy 0.62) and **9<sub>eq</sub>** (occupancy 0.38) with axial and equatorial orientation of the diazaphospholene ligand, respectively (from left to right). For clarity, hydrogen atoms were omitted and N-Dipp substituents represented using a wire model. Thermal ellipsoids in the representations of **9<sub>ax</sub>** and **9<sub>eq</sub>** were drawn at the 50% probability level.

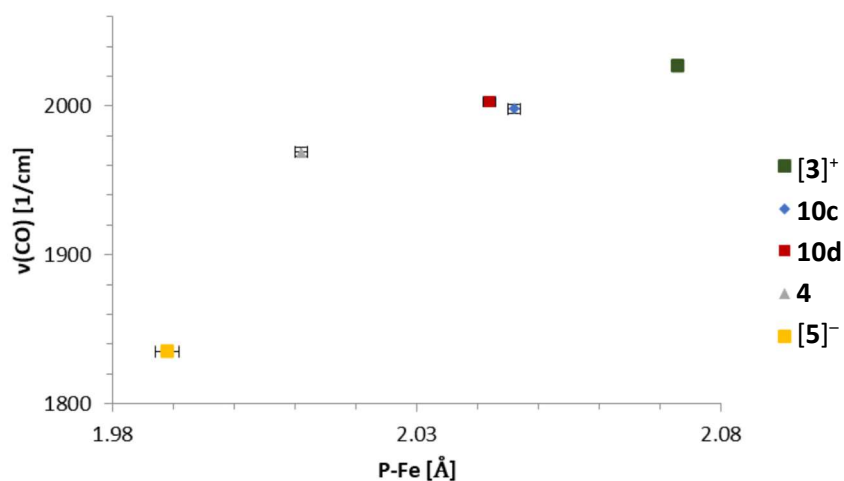


**Figure S3.** Correlation of the wavenumbers of the midmost IR-active  $\nu_{\text{CO}}$ -mode with the P–Fe distances for complexes  $[(^{\text{Dipp}}\text{PNHP})\text{Fe}(\text{CO})_3(\text{Do})]^+$  (Do = CO (**[3]<sup>+</sup>**), Br<sup>−</sup> (**10c**), I<sup>−</sup> (**10d**), H<sup>−</sup> (**4**), 2 e<sup>−</sup> (**[5]<sup>−</sup>**)). Error bars correspond to the esds for P–Fe and were estimated as  $\pm 3 \text{ cm}^{-1}$  for  $\nu_{\text{CO}}$ .

## EPR Spectra

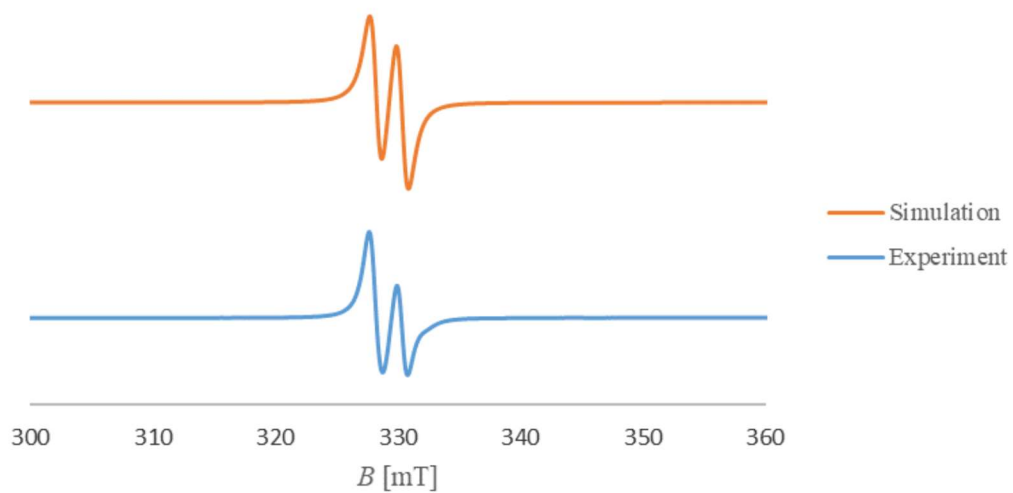


**Figure S4.** Observed (blue trace) and simulated (orange trace) X-band EPR spectrum of the reaction of [3]OTf with LDA in THF. Simulation parameters:  $S = \frac{1}{2}$ ,  $g = 2.052$ ,  $A(^{31}\text{P}) = 61.2$  MHz (2.18 mT),  $lwppG = 0.27$  mT,  $lwppL = 0.98$  mT.

## NMR spectra

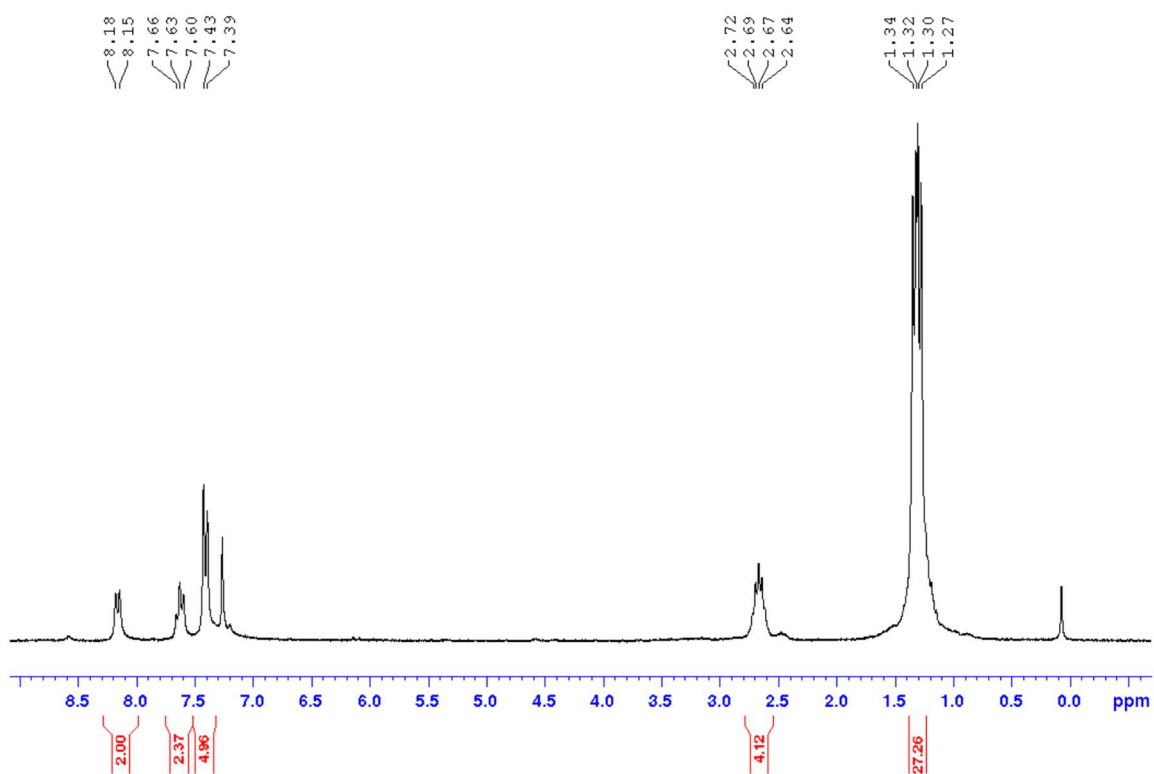


**Figure S5.**  $^1\text{H}$  NMR spectrum of [3]OTf in  $\text{CDCl}_3$ .

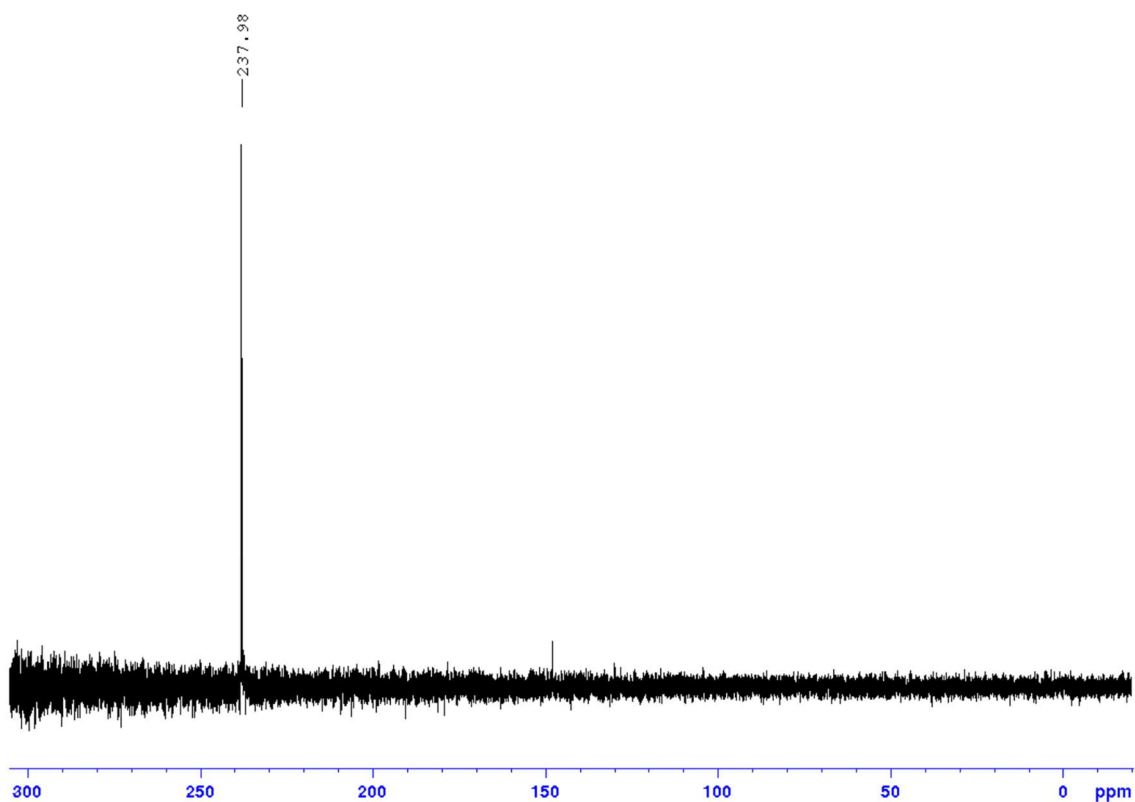


Figure S6.  $^{31}\text{P}\{^1\text{H}\}$  NMR spectrum of [3]OTf in  $\text{CDCl}_3$ .

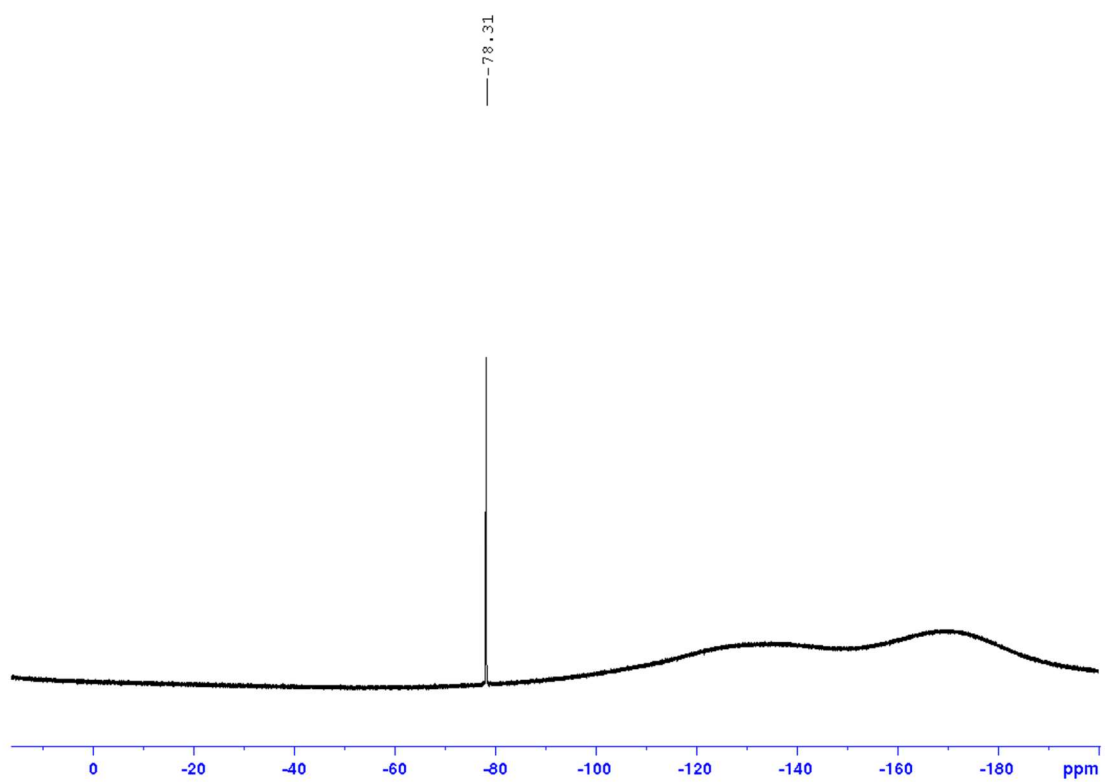
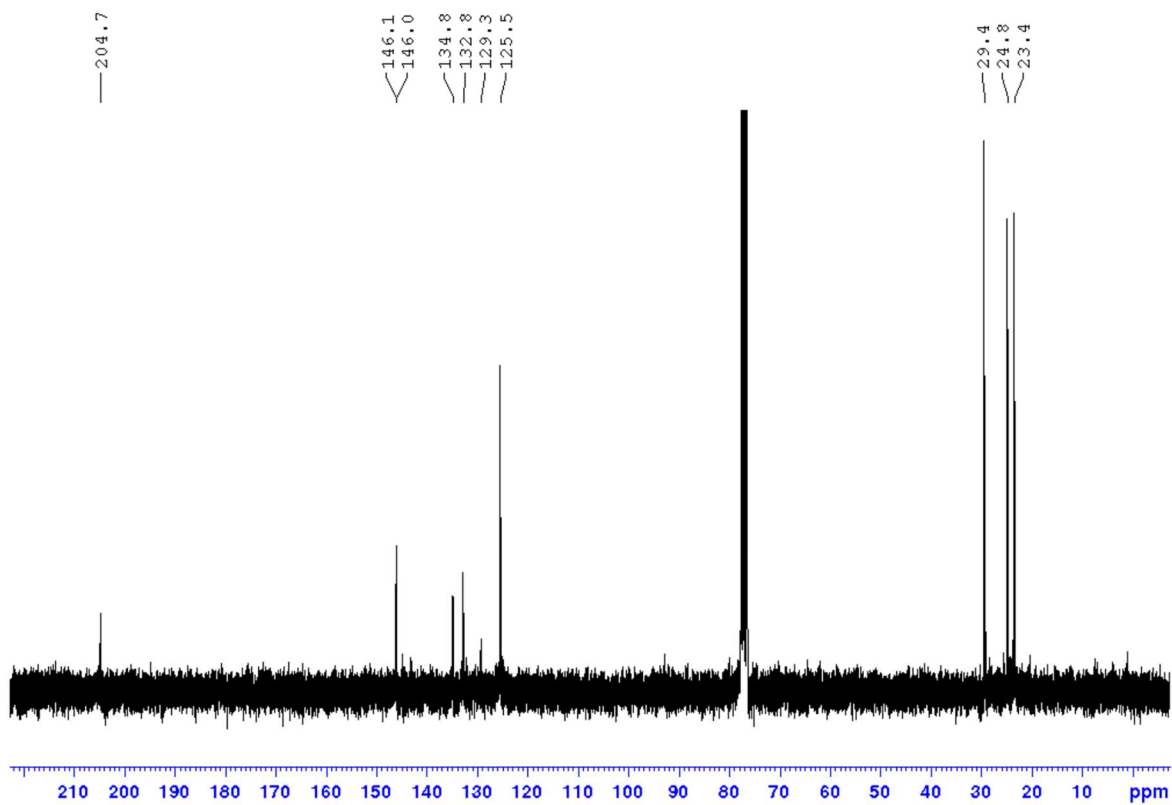
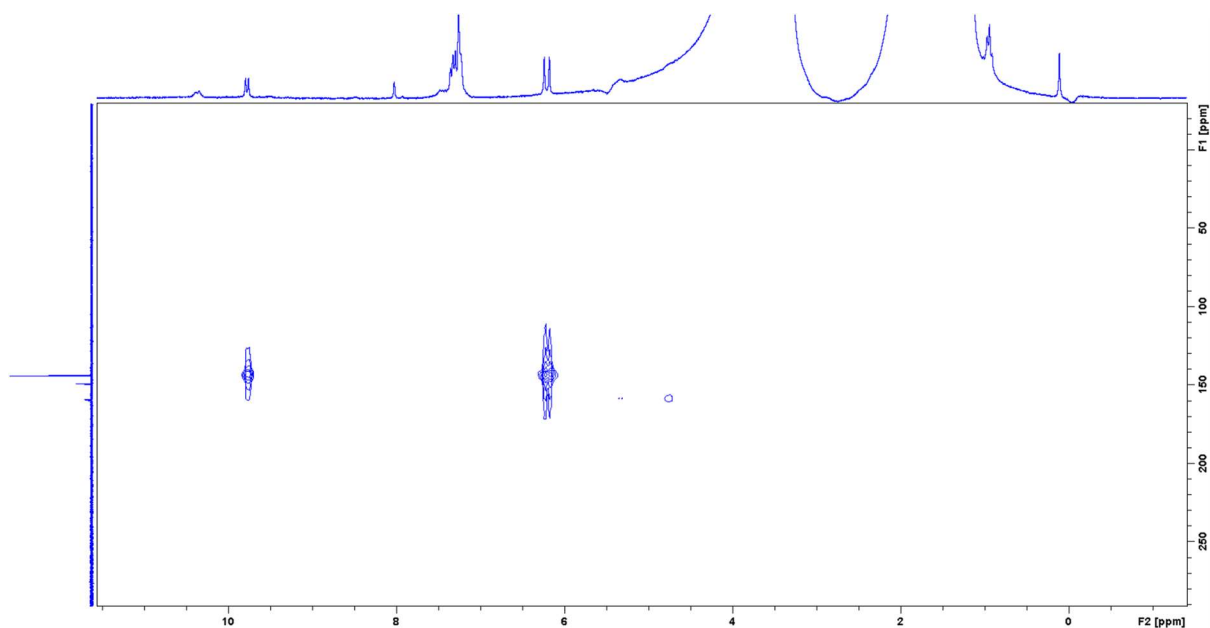


Figure S7.  $^{19}\text{F}$  NMR spectrum of [3]OTf in  $\text{CDCl}_3$ .



**Figure S8.**  $^{13}\text{C}\{^1\text{H}\}$  NMR spectrum of [3]OTf in  $\text{CDCl}_3$ .



**Figure S9.** Two-dimensional  $^1\text{H},^{31}\text{P}$  HMQC NMR spectrum of a solution of [3]OTf in moist THF. The correlation signals are attributable to **6**.

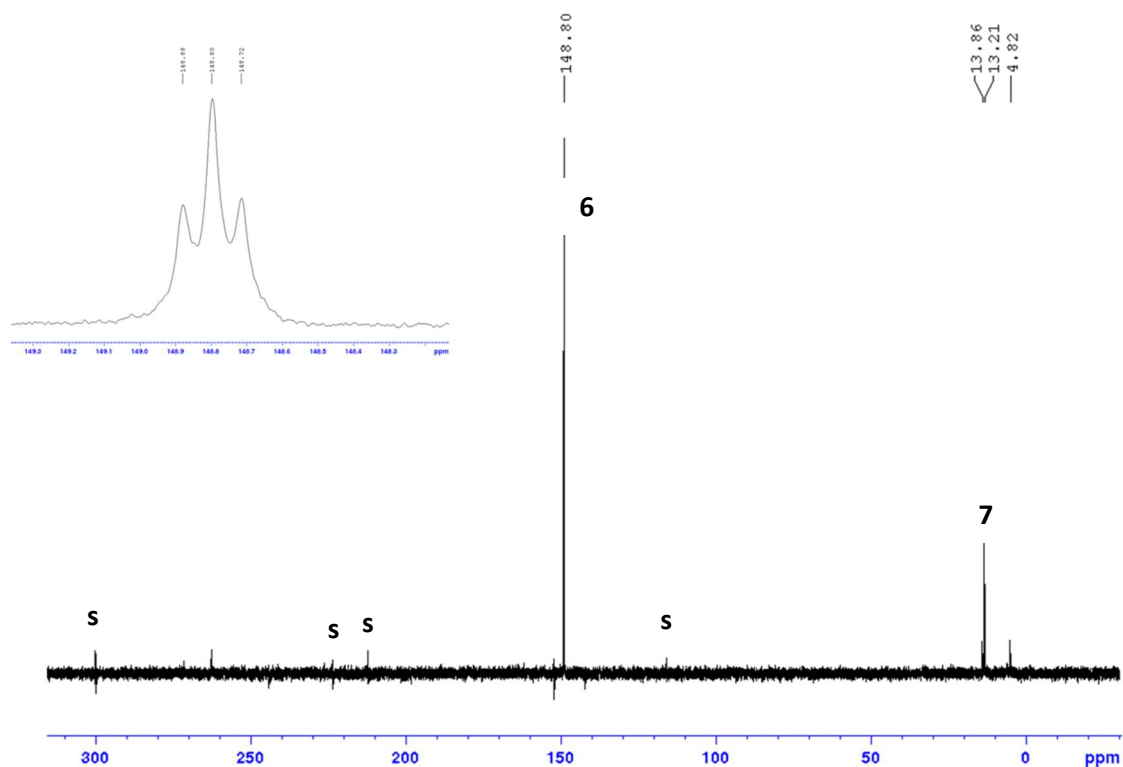


**Figure S10.**  $^{31}\text{P}\{^1\text{H}\}$  NMR spectrum and expansion of the  $^{31}\text{P}$  NMR spectrum (insert) of the crude product obtained after dissolution of [3]OTf in moist THF, evaporation of the solvent, and redissolution in  $\text{C}_6\text{D}_6$ . The labels denote signals attributable to **6** and **7** and electronic spikes (s). The insert displays an expansion of the signal of **6** in the  $^{31}\text{P}$  NMR spectrum. The splitting is attributable to spin coupling with the  $^1\text{H}$  nuclei on the NHP ring while the coupling to the OH proton is ostensibly quenched by intermolecular chemical exchange.

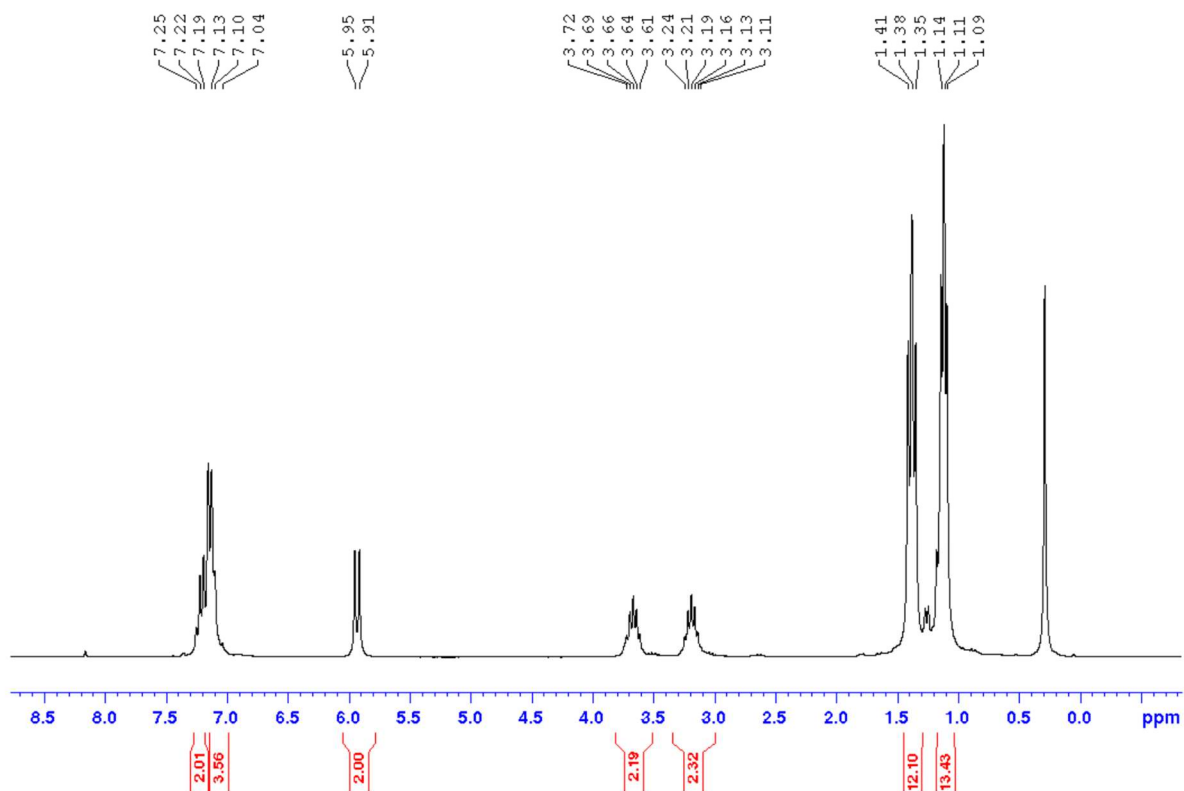


**Figure S11.**  $^1\text{H}$  NMR spectrum of **8a** in  $\text{C}_6\text{D}_6$ .

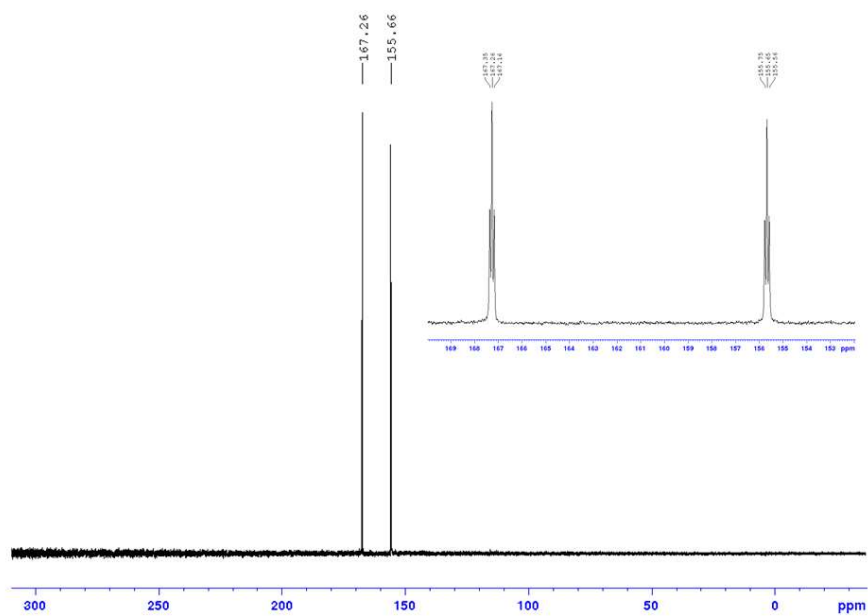


**Figure S12.**  $^{31}\text{P}\{^1\text{H}\}$  NMR spectrum of **8a** in  $\text{C}_6\text{D}_6$ . The insert shows the expanded signal in the  $^{31}\text{P}$  NMR spectrum.

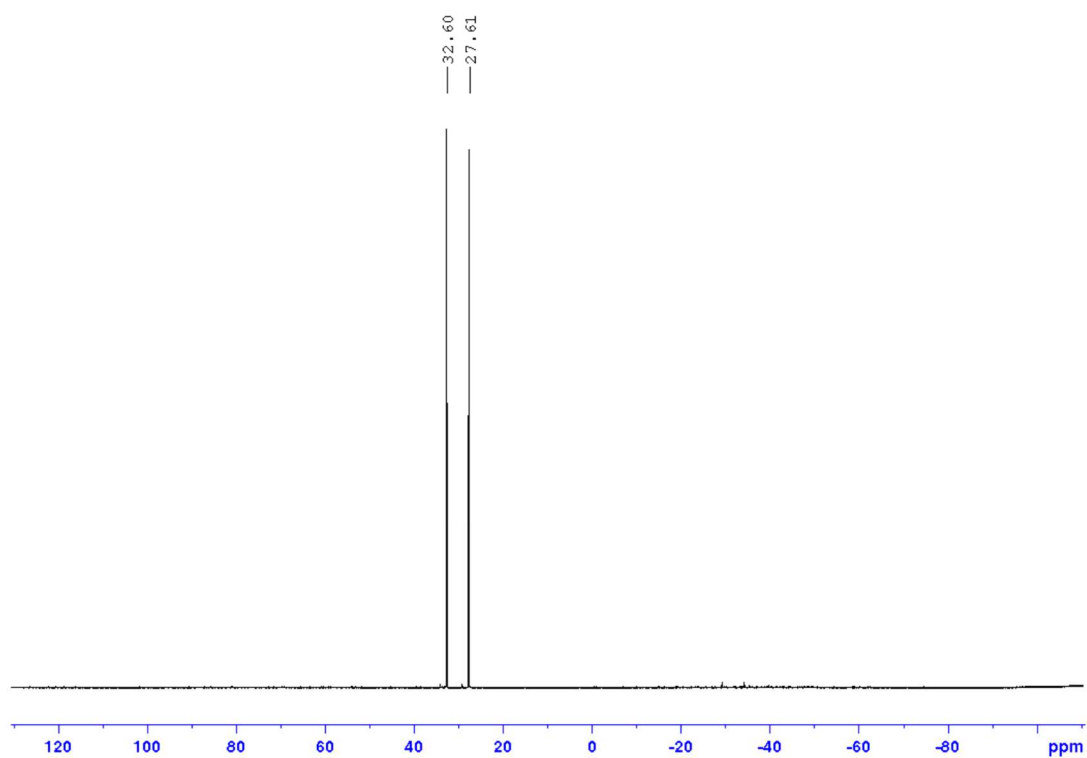


**Figure S13.**  $^{19}\text{F}$  NMR spectrum of **8a** in  $\text{C}_6\text{D}_6$ .

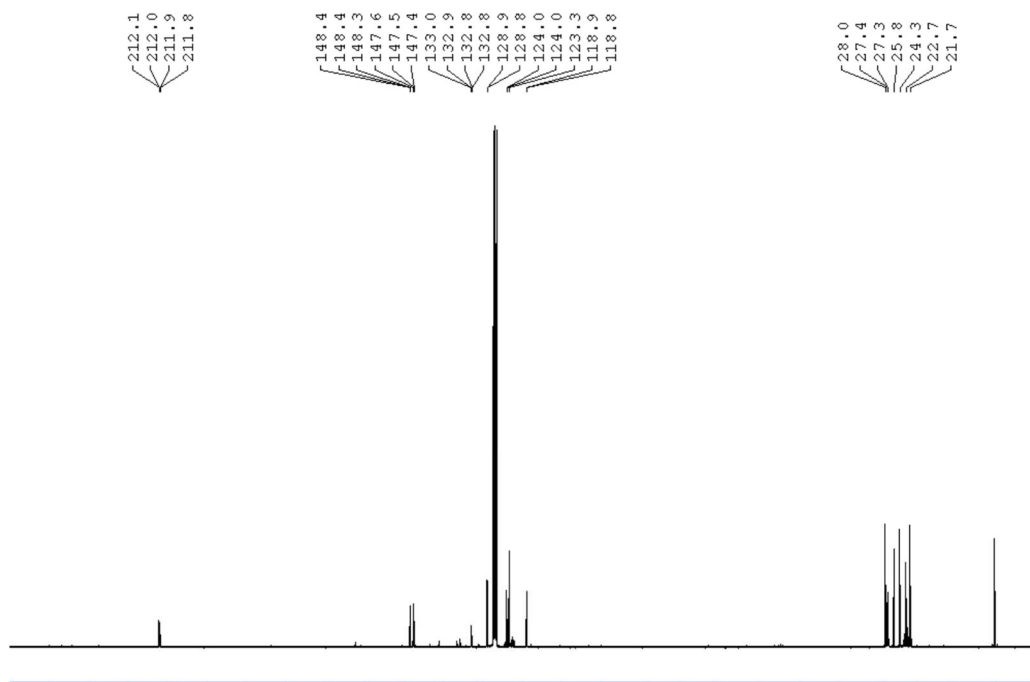


Figure S14.  $^{13}\text{C}\{^1\text{H}\}$  NMR spectrum of **8a** in  $\text{C}_6\text{D}_6$ .

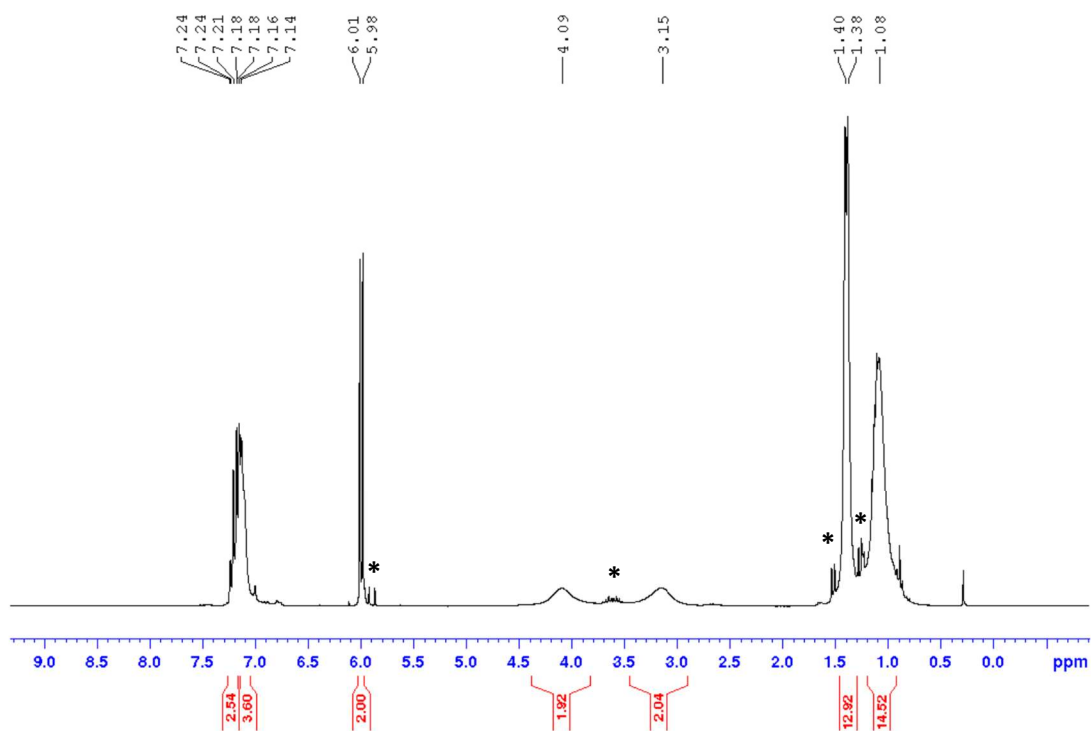
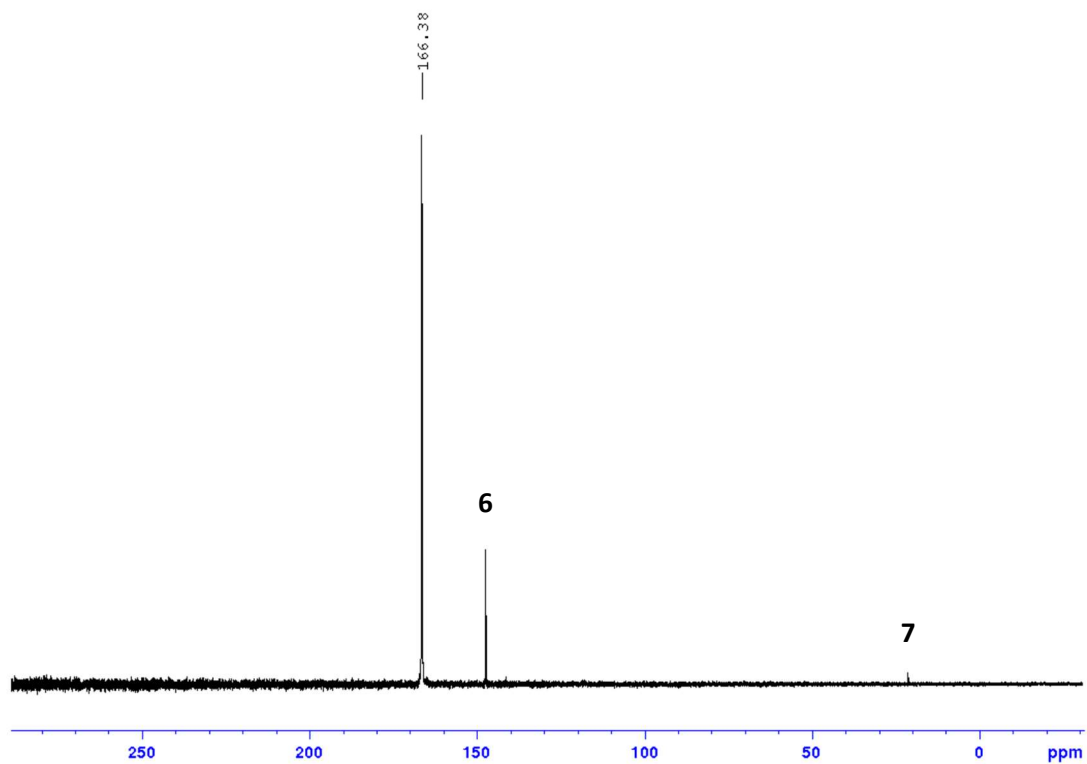
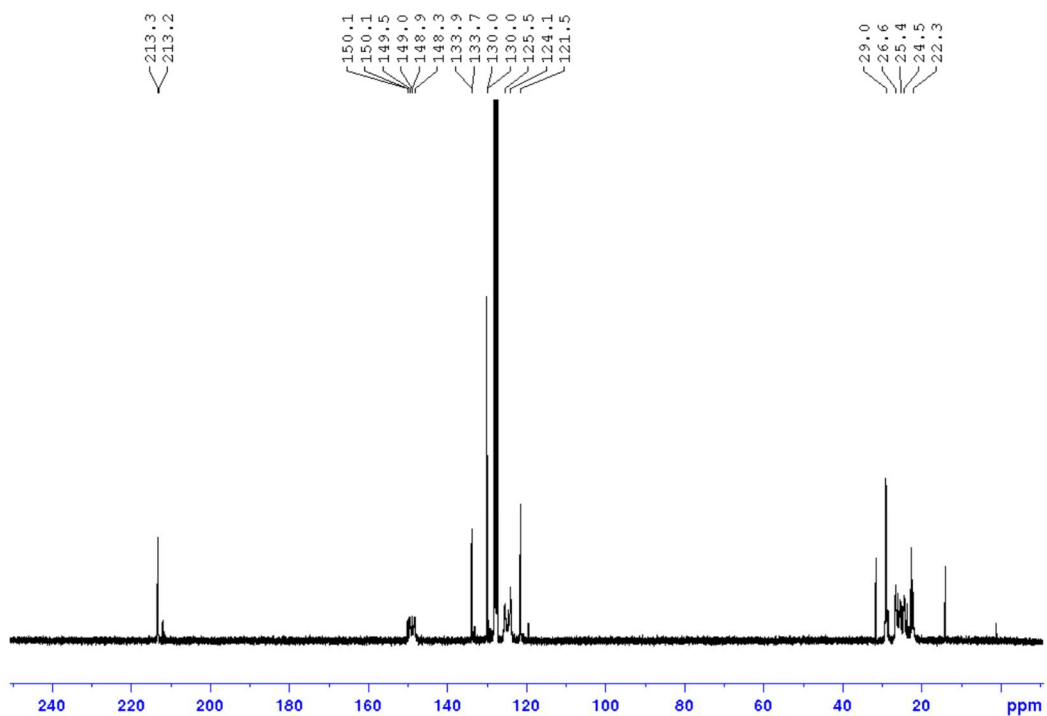


Figure S15.  $^1\text{H}$  NMR spectrum of **8b** in  $\text{C}_6\text{D}_6$ . The signals labelled with an asterisk denote signals of **6** and **7** arising from partial hydrolysis during sample preparation. The broadening of some signals arises from intermolecular exchange of Cl-atoms.



**Figure S16.**  $^{31}\text{P}\{^1\text{H}\}$  NMR spectrum of **8b** in  $\text{C}_6\text{D}_6$ . The additional signals attributable to **6** and **7** arising from partial hydrolysis during sample preparation.



**Figure S17.**  $^{13}\text{C}\{^1\text{H}\}$  NMR spectrum of **8b** in  $\text{C}_6\text{D}_6$ .



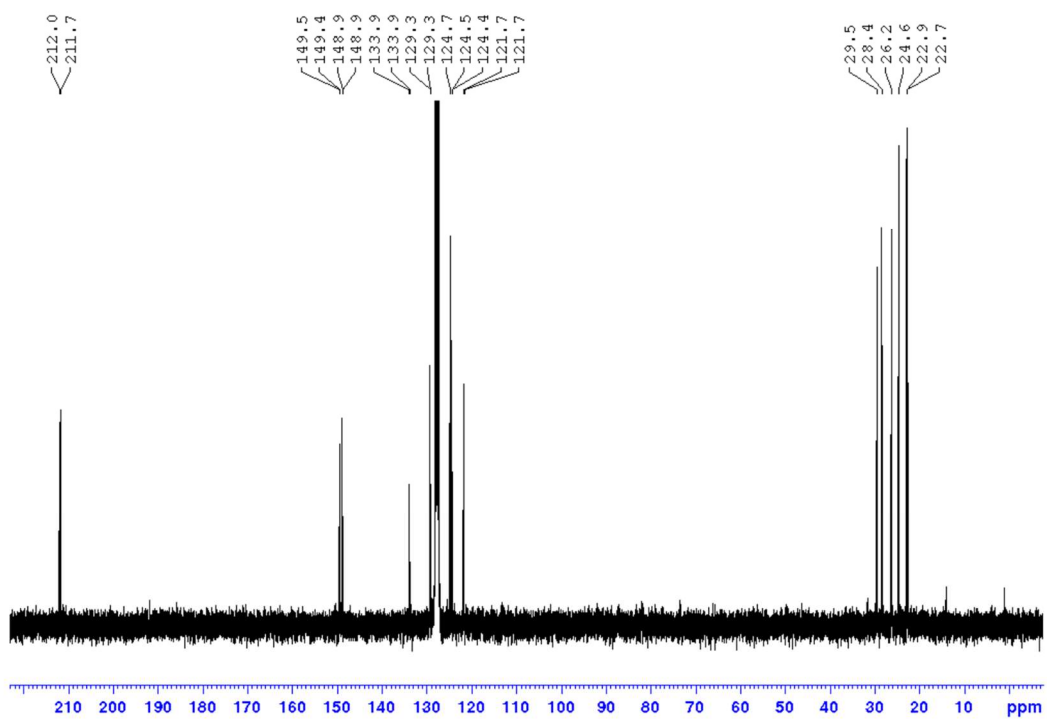


Figure S20.  $^{13}\text{C}\{^1\text{H}\}$  NMR spectrum of **9** in  $\text{C}_6\text{D}_6$ .

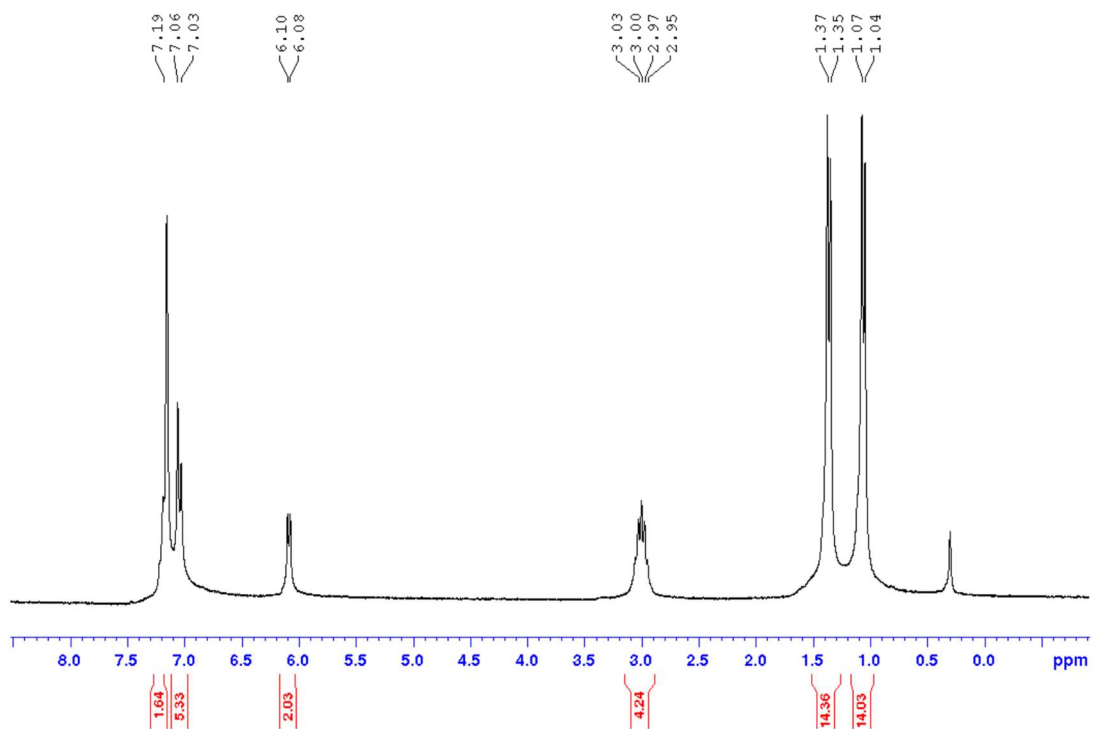


Figure S21.  $^1\text{H}$  NMR spectrum of **10c** in  $\text{C}_6\text{D}_6$ .

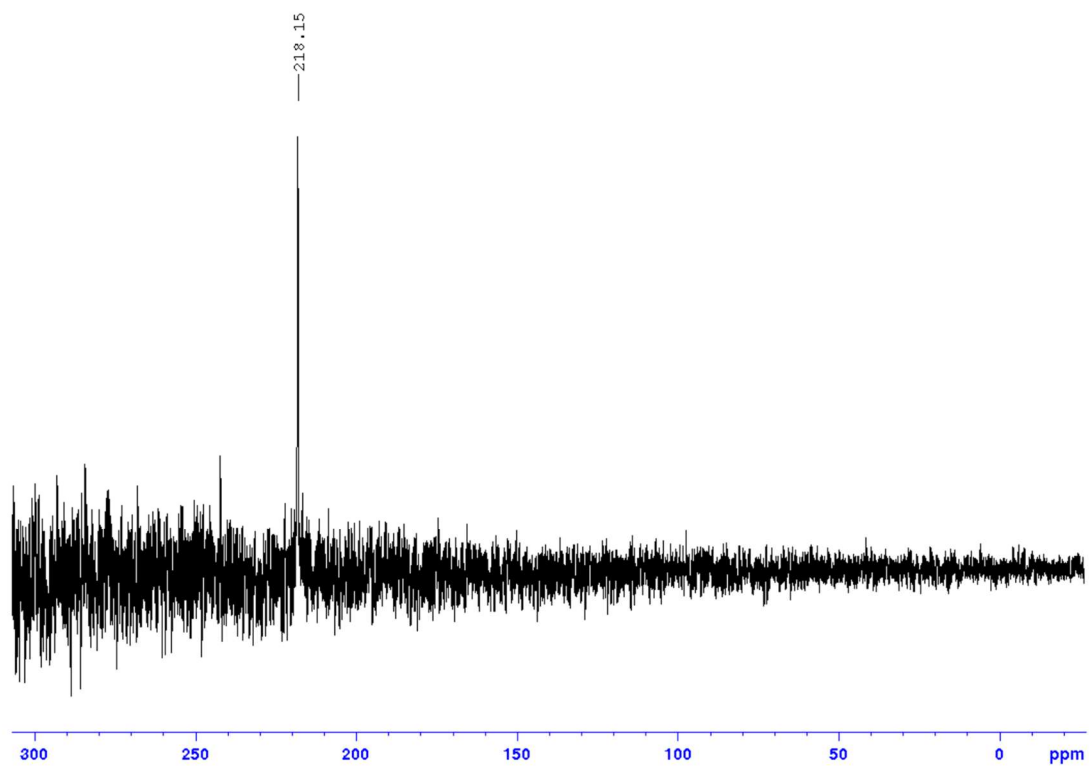


Figure S22.  $^{31}\text{P}\{^1\text{H}\}$  NMR spectrum of **10c** in  $\text{C}_6\text{D}_6$ .

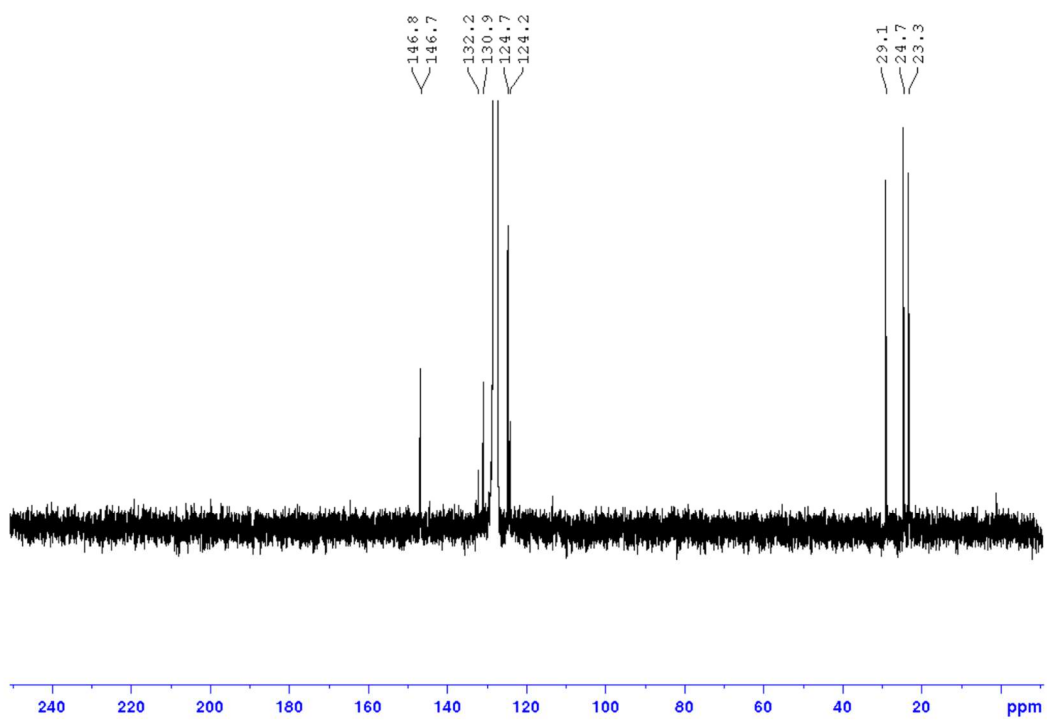


Figure S23.  $^{13}\text{C}\{^1\text{H}\}$  NMR spectrum of **10c** in  $\text{C}_6\text{D}_6$ .

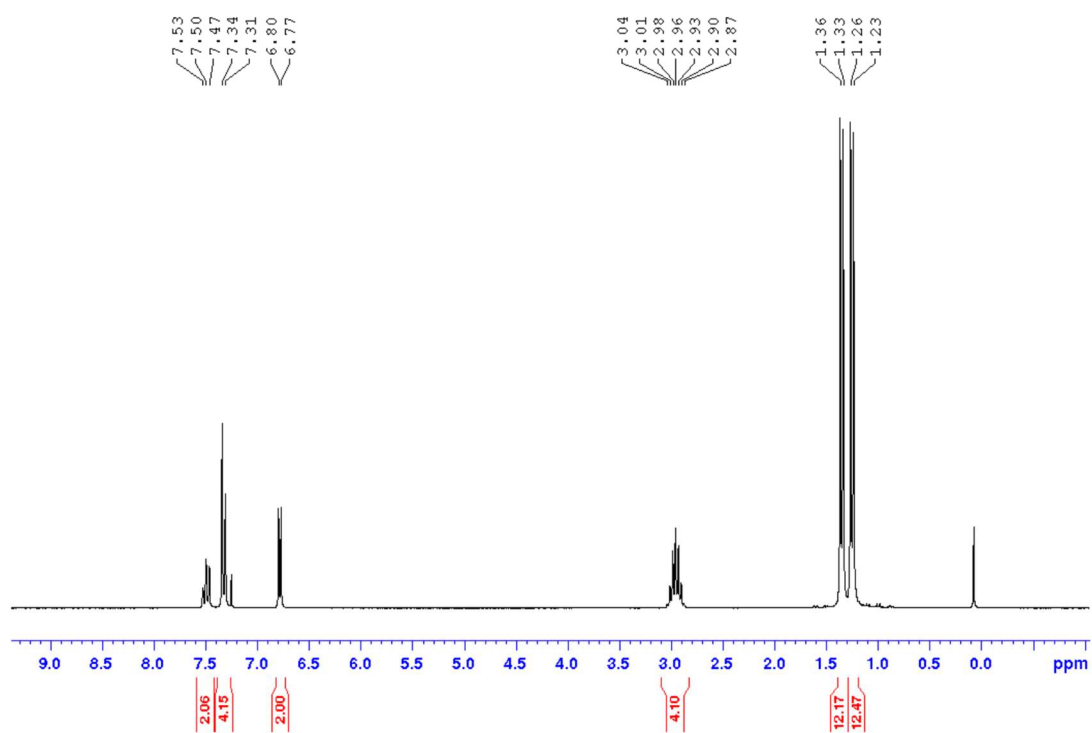


Figure S24.  $^1\text{H}$  NMR spectrum of **10d** in  $\text{C}_6\text{D}_6$ .

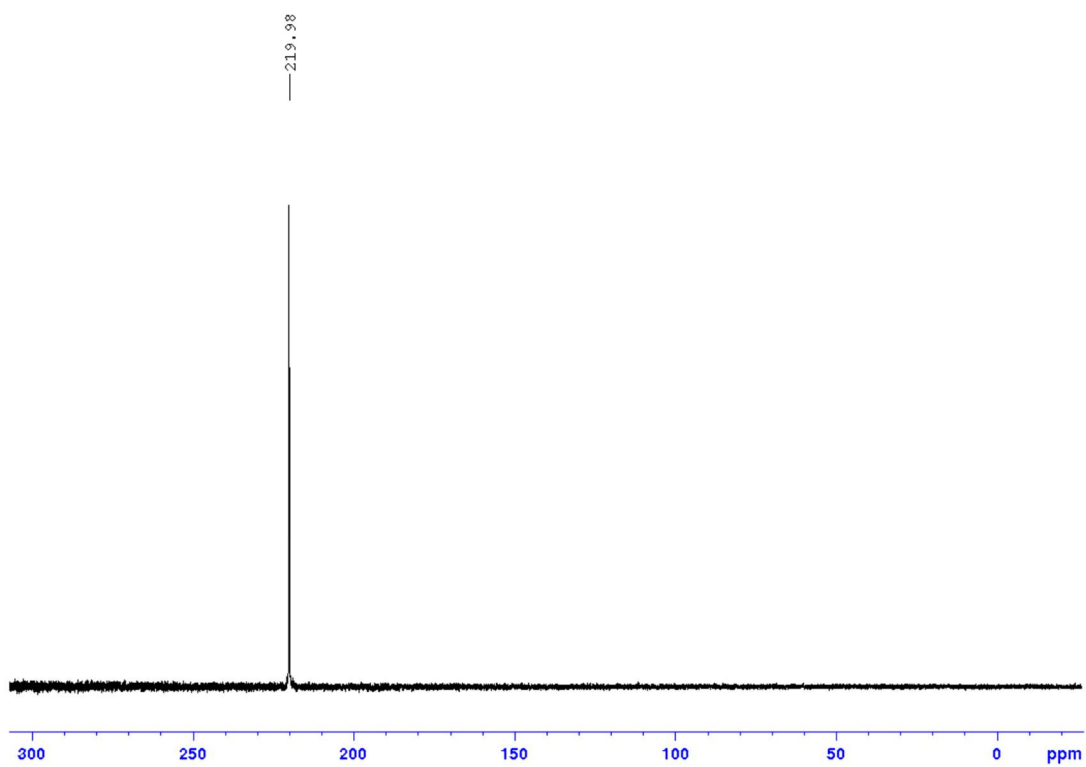


Figure S25.  $^{31}\text{P}\{^1\text{H}\}$  NMR spectrum of **10d** in  $\text{C}_6\text{D}_6$ .

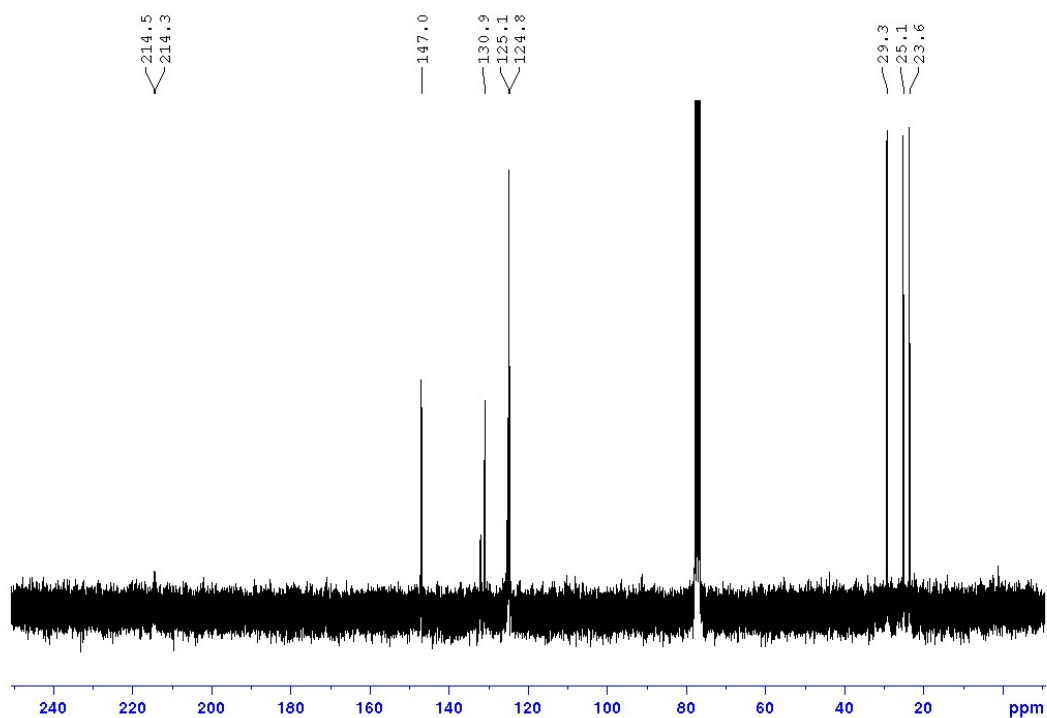


Figure S26.  $^{13}\text{C}\{^1\text{H}\}$  NMR spectrum of **10d** in  $\text{C}_6\text{D}_6$ .

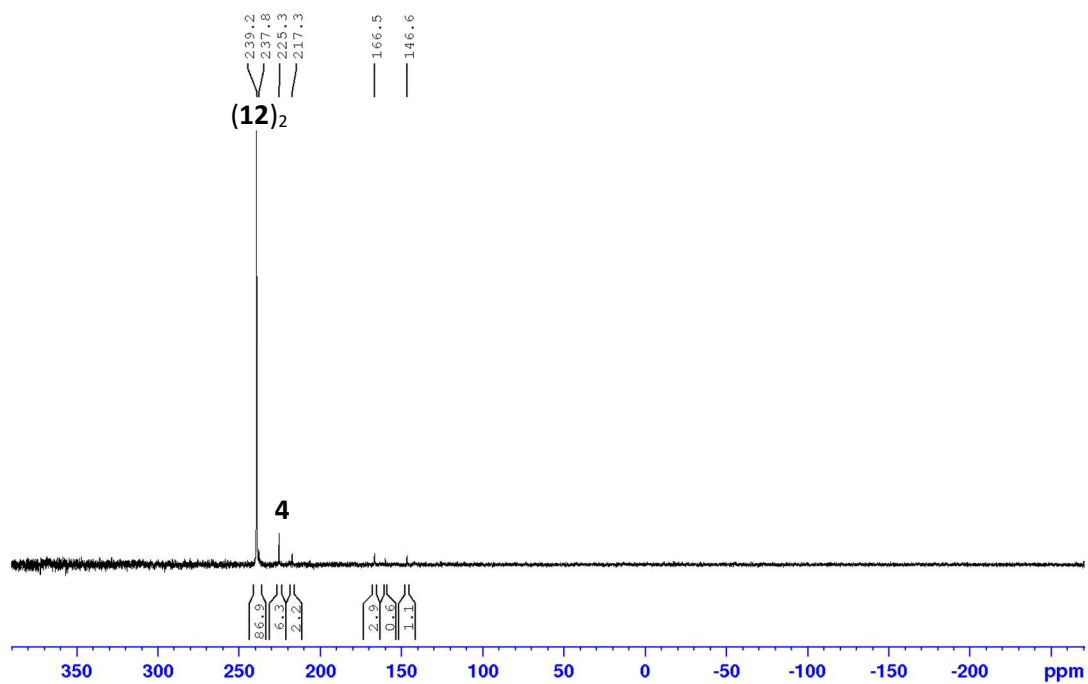
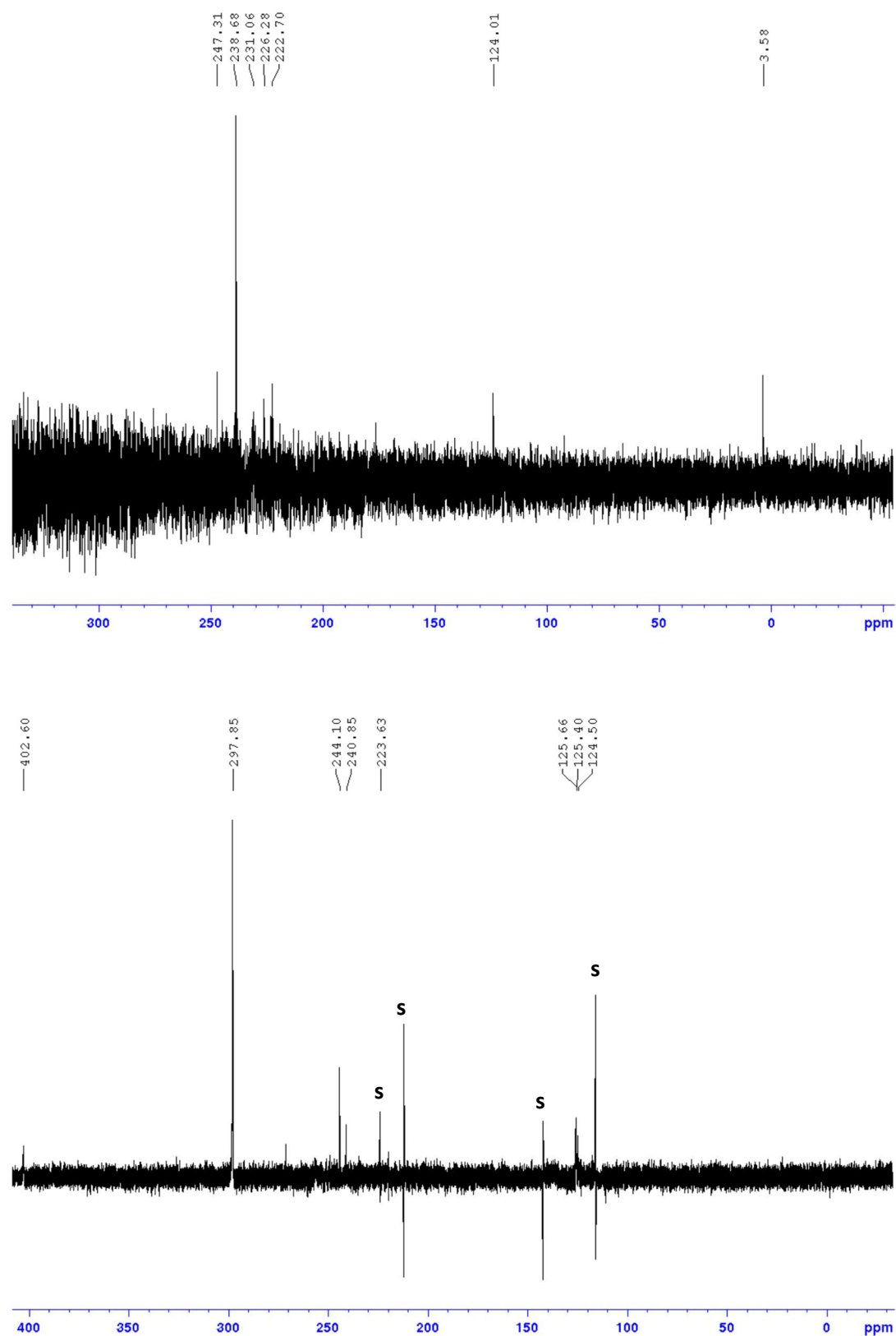


Figure S27.  $^{31}\text{P}\{^1\text{H}\}$  NMR spectrum of the reaction of **17b** with 1.5 equiv. of  $[(\text{ba})\text{Fe}(\text{CO})_3]$  at  $40\text{ }^\circ\text{C}$  in toluene with assignment of the signals of **(12)<sub>2</sub>** (87%) and **4** (6%).



**Figure S28.**  $^{31}\text{P}\{^1\text{H}\}$  NMR spectra of the reaction of [3]OTf with LDA in THF at room temperature (top trace) and at  $-78\text{ }^\circ\text{C}$  (bottom trace). Signals labelled with "s" are electronic spikes. Note the different horizontal scales of both spectra.

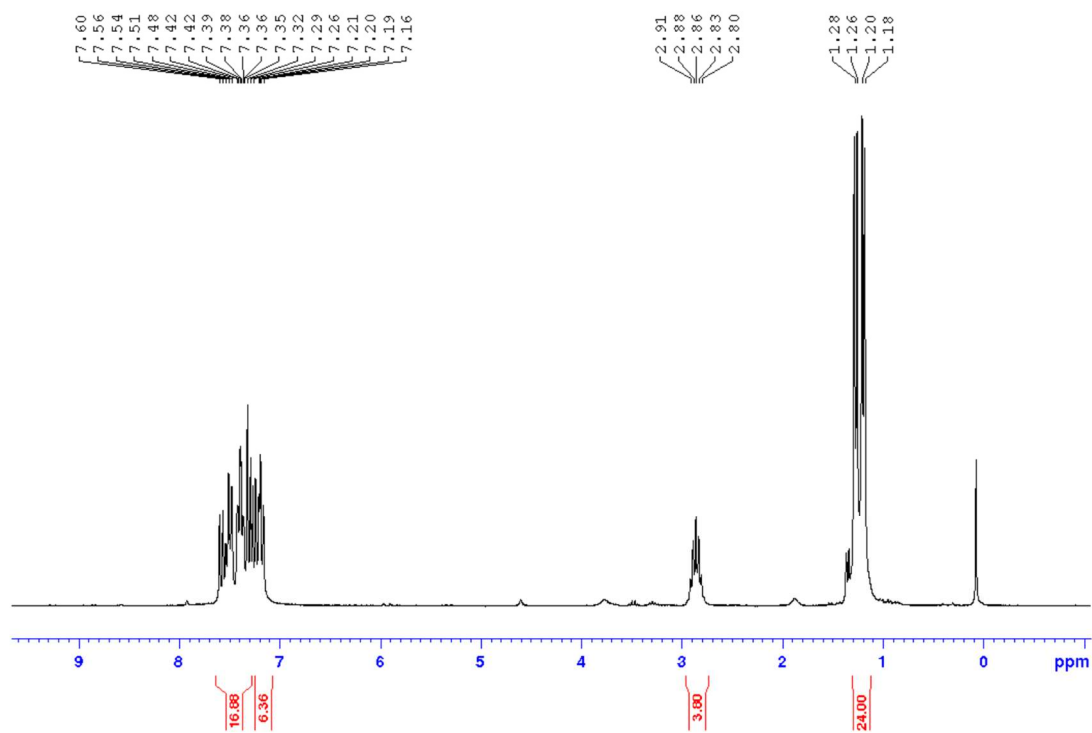


Figure S29.  $^1\text{H}$  NMR spectrum of [15]OTf in  $\text{CDCl}_3$ .

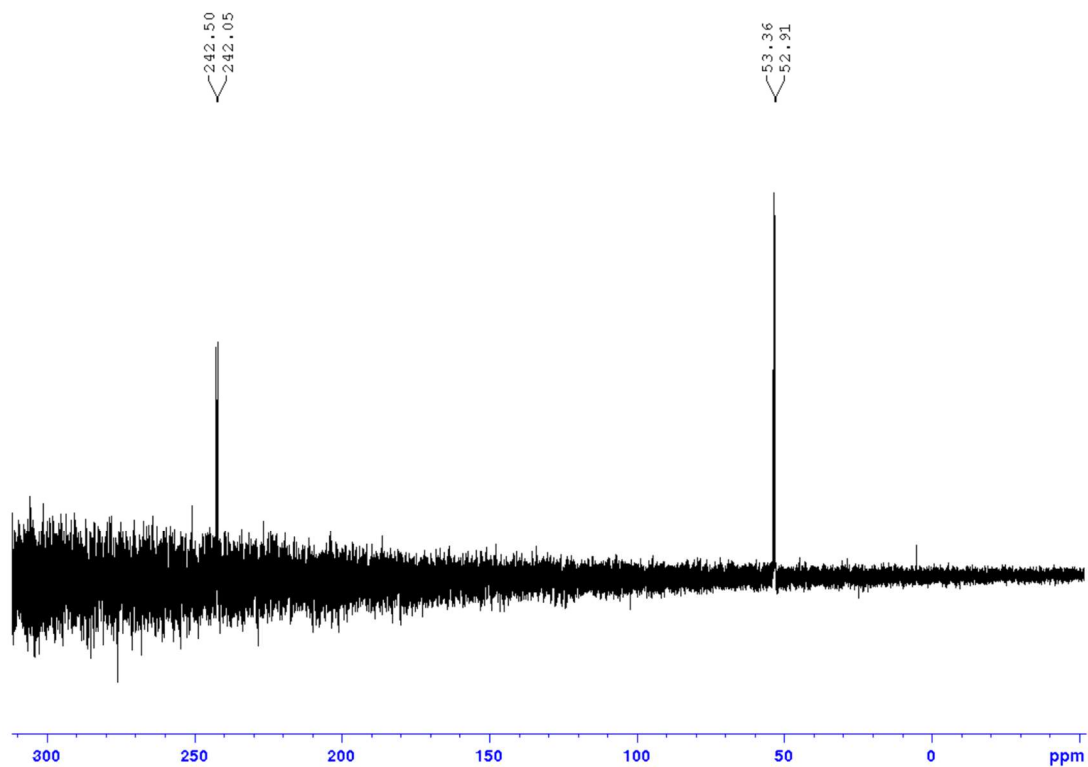


Figure S30.  $^{31}\text{P}\{^1\text{H}\}$  NMR spectrum of [15]OTf in  $\text{CDCl}_3$ .

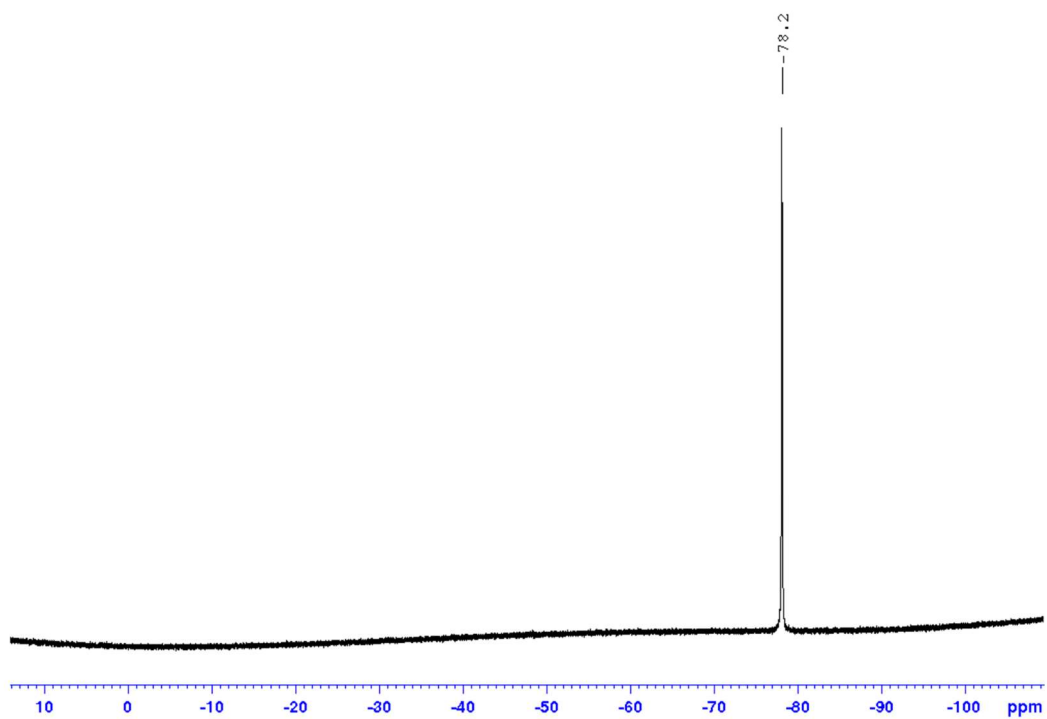


Figure S31.  $^{19}\text{F}$  NMR spectrum of [15]OTf in  $\text{CDCl}_3$ .

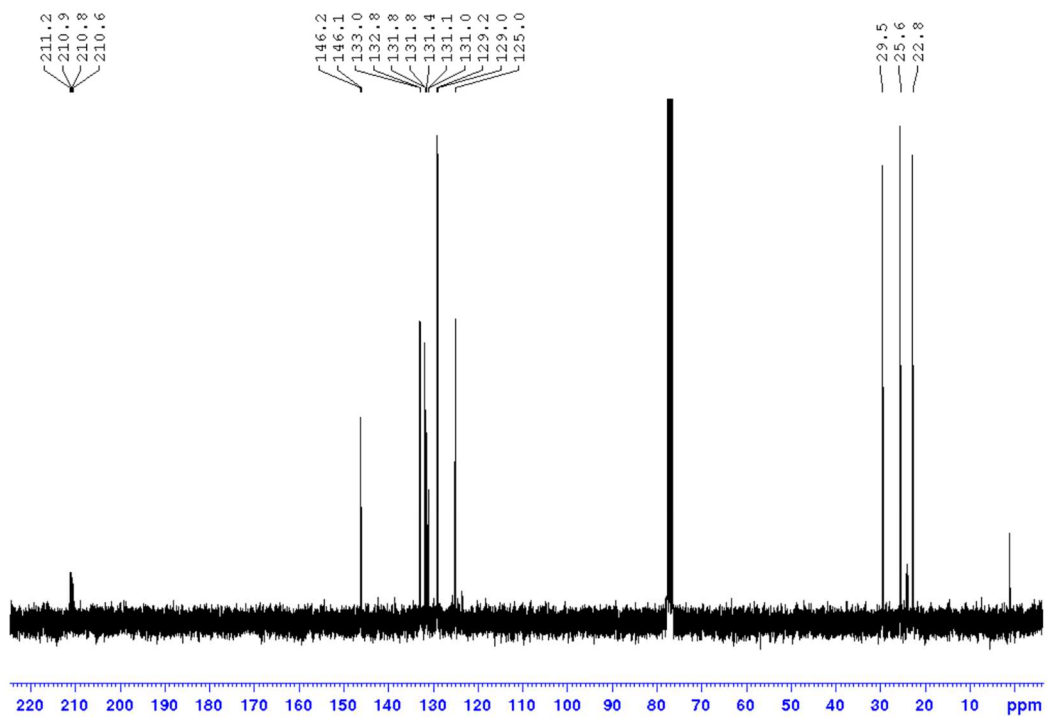
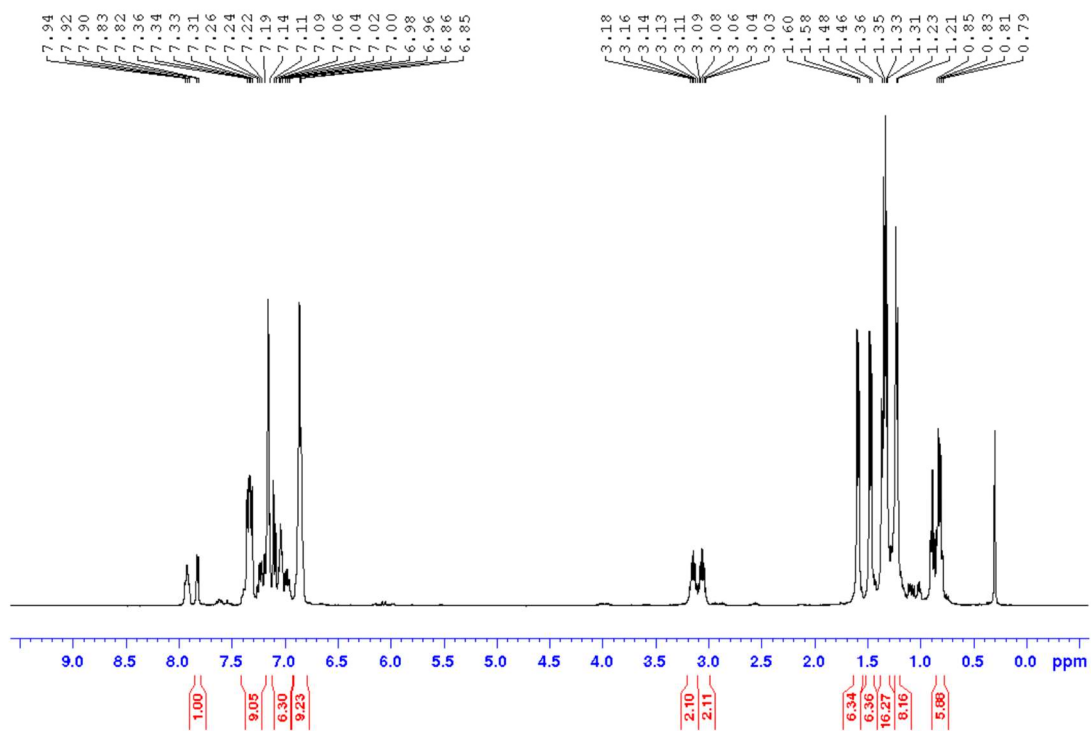
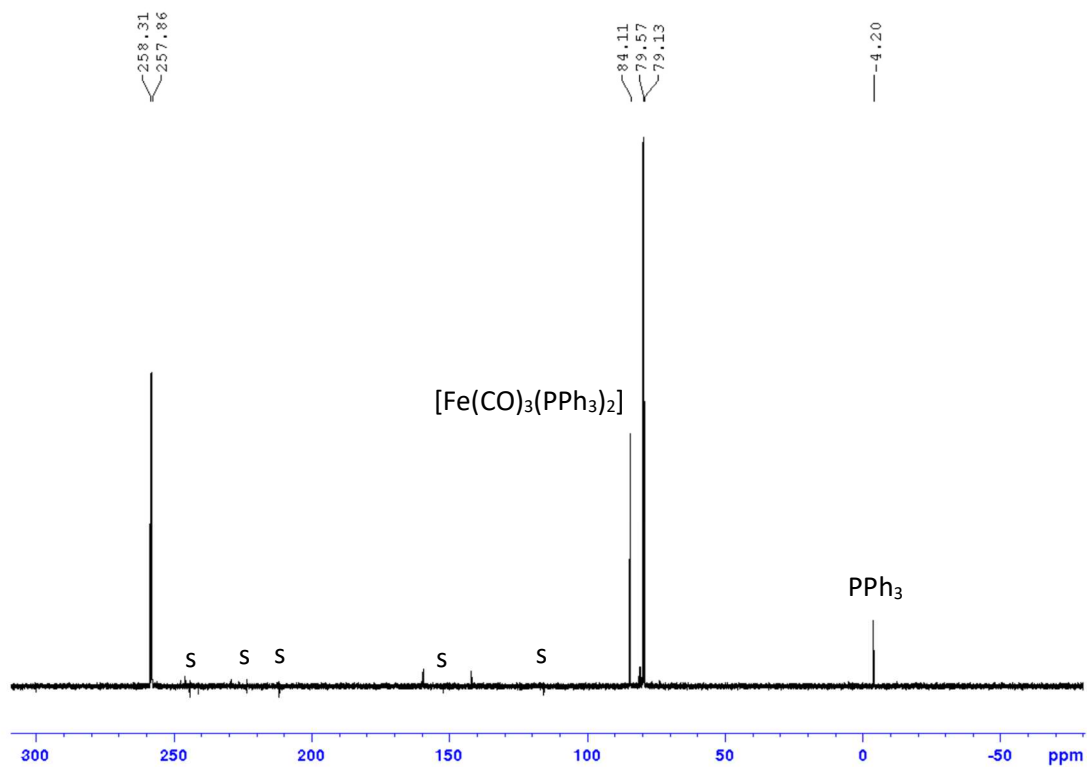


Figure S32.  $^{13}\text{C}\{^1\text{H}\}$  NMR spectrum of [15]OTf in  $\text{CDCl}_3$ .



**Figure S33.**  $^1\text{H}$  NMR spectrum of crude **16** in  $\text{C}_6\text{D}_6$ .



**Figure S34.**  $^{31}\text{P}\{^1\text{H}\}$  NMR spectrum of crude **16** in  $\text{C}_6\text{D}_6$ . Labels denote signals attributable to impurities and electronic spikes (s).

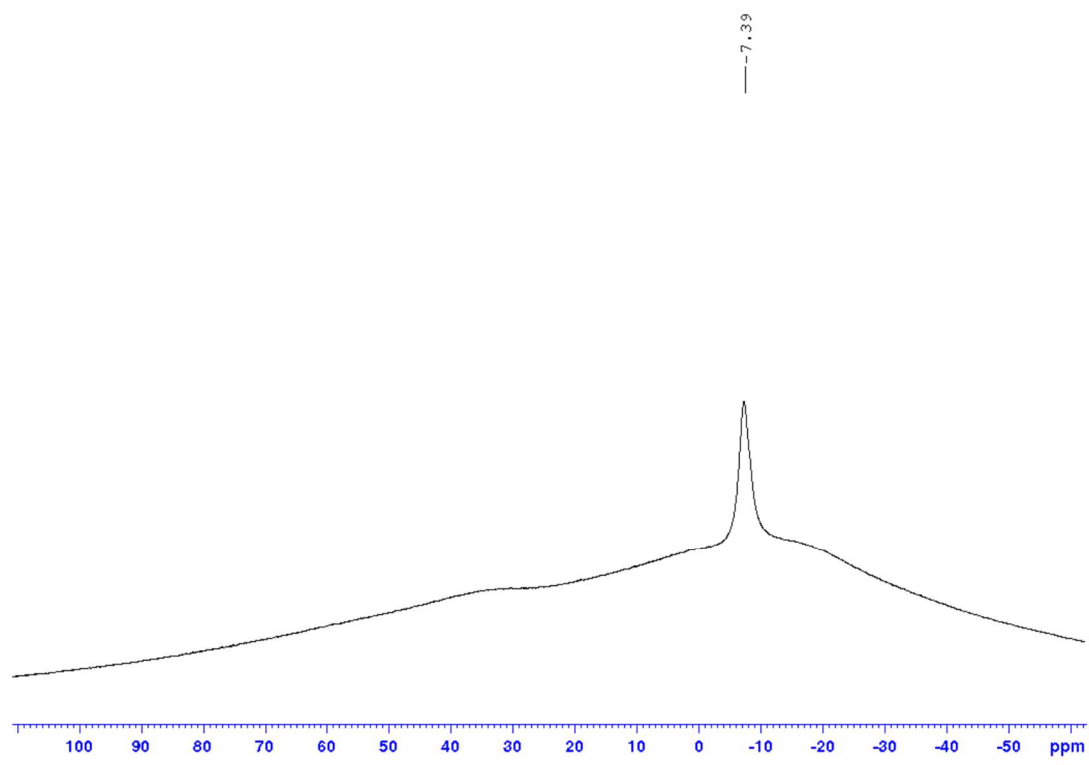


Figure S35. <sup>11</sup>B NMR spectrum of crude **16** in C<sub>6</sub>D<sub>6</sub>.

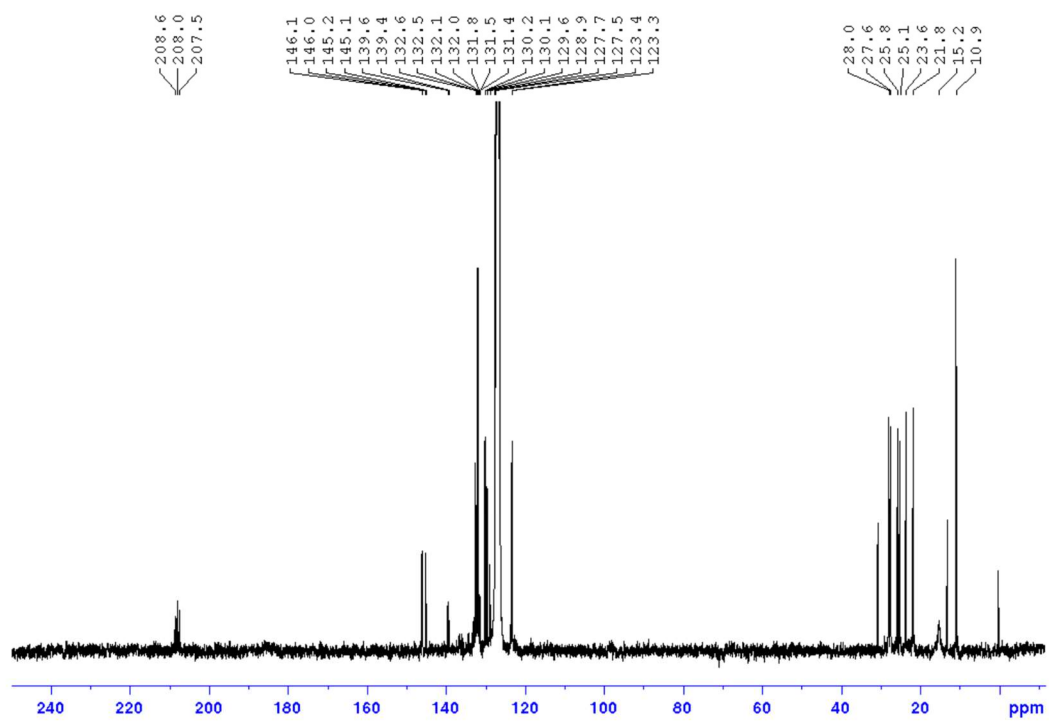


Figure S36. <sup>13</sup>C{<sup>1</sup>H} NMR spectrum of crude **16** in C<sub>6</sub>D<sub>6</sub>.

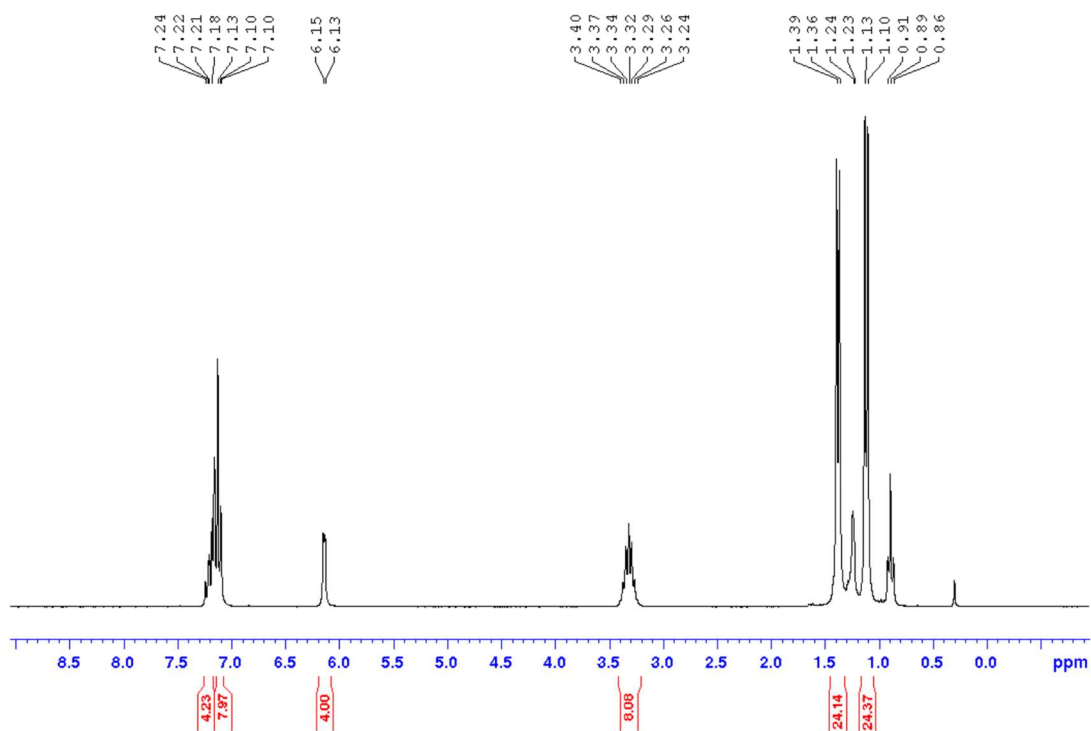


Figure S37.  $^1\text{H}$  NMR spectrum of  $(\mathbf{12})_2$  in  $\text{C}_6\text{D}_6$ .

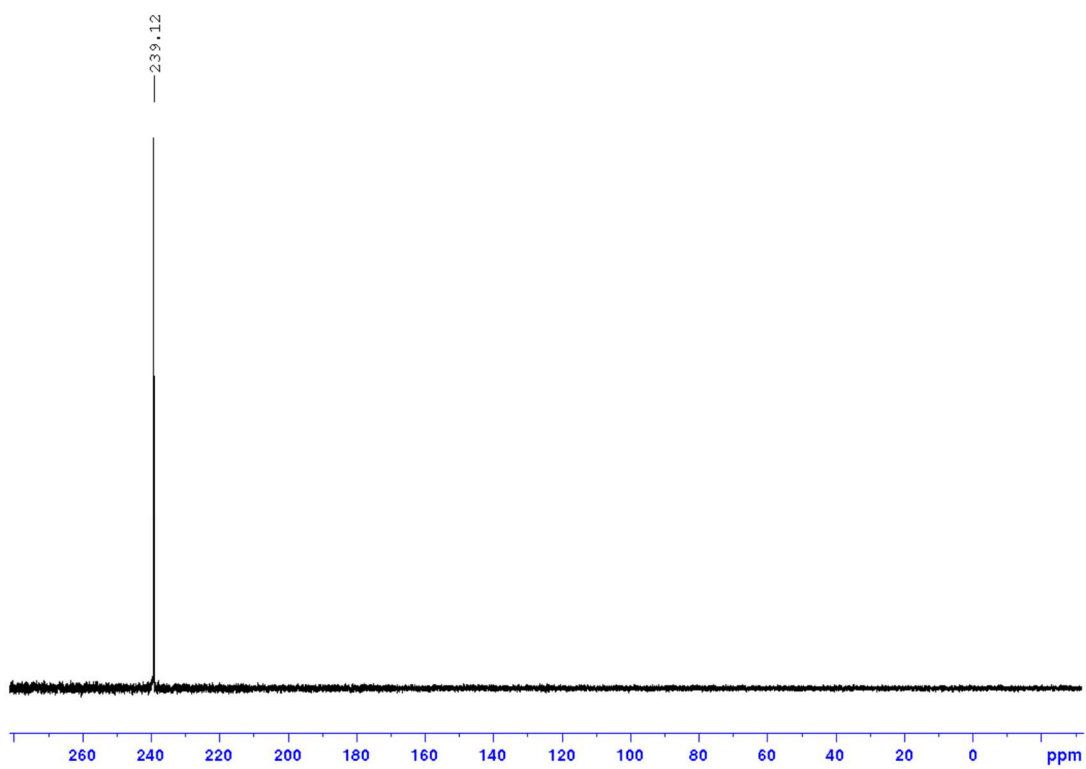


Figure S38.  $^{31}\text{P}\{^1\text{H}\}$  NMR spectrum of  $(\mathbf{12})_2$  in  $\text{C}_6\text{D}_6$ .

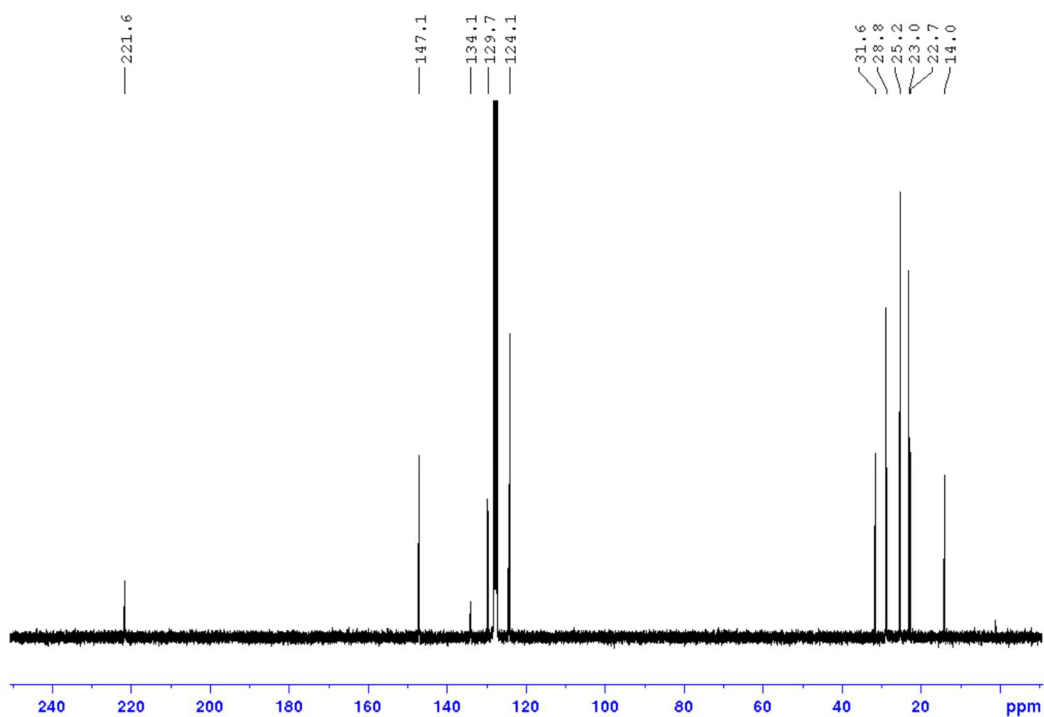


Figure S39.  $^{13}\text{C}\{^1\text{H}\}$  NMR spectrum of  $(\mathbf{12})_2$  in  $\text{C}_6\text{D}_6$ .

### FTIR Spectra

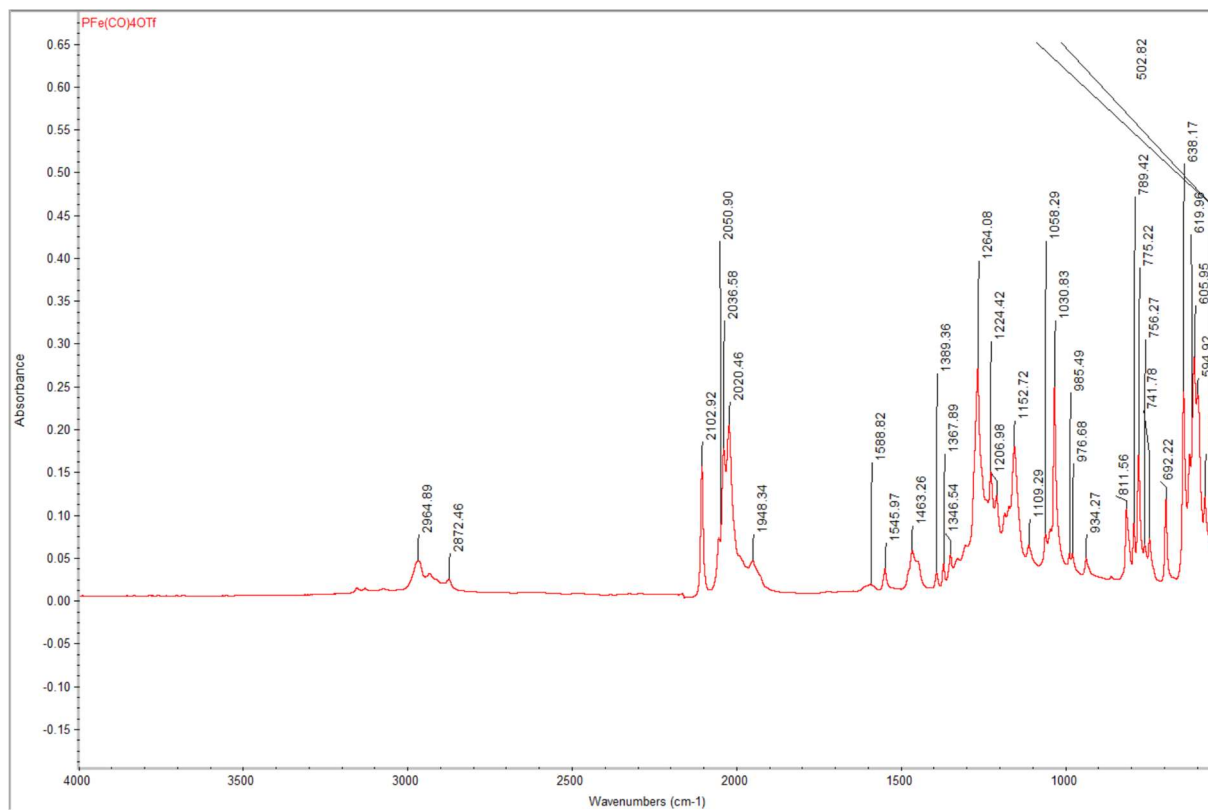


Figure S40. FTIR spectrum of  $[\mathbf{3}]\text{OTf}$ .

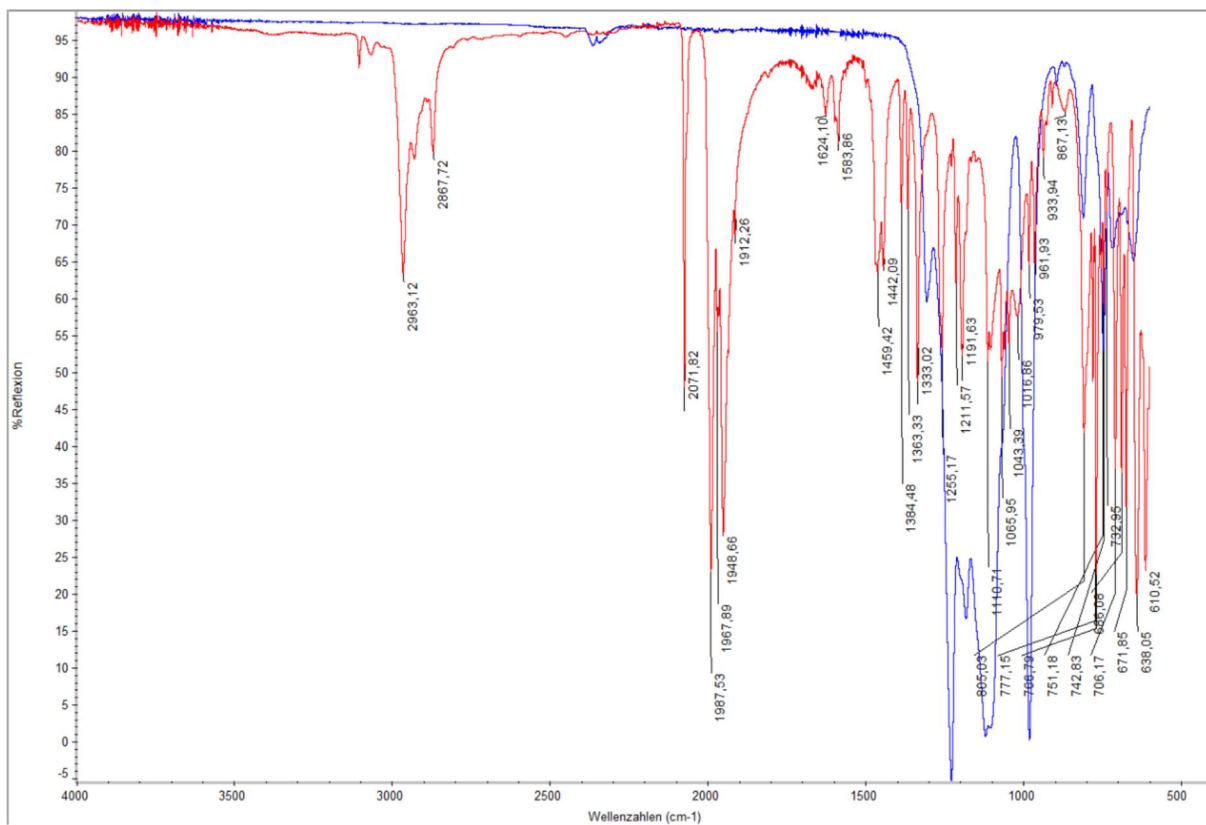


Figure S41. FTIR spectrum of 8a in Fomblin Y oil (red trace) and background spectrum of the oil (blue trace).

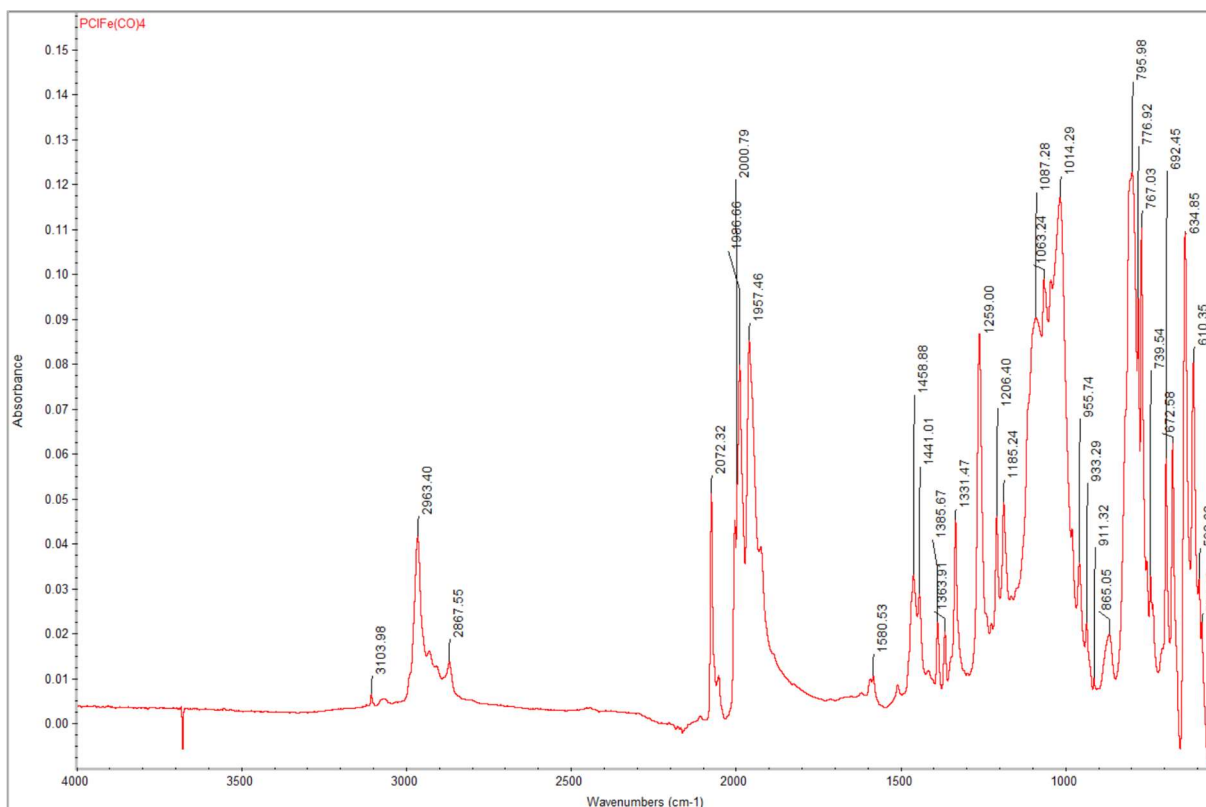


Figure S42. FTIR spectrum of 8b.

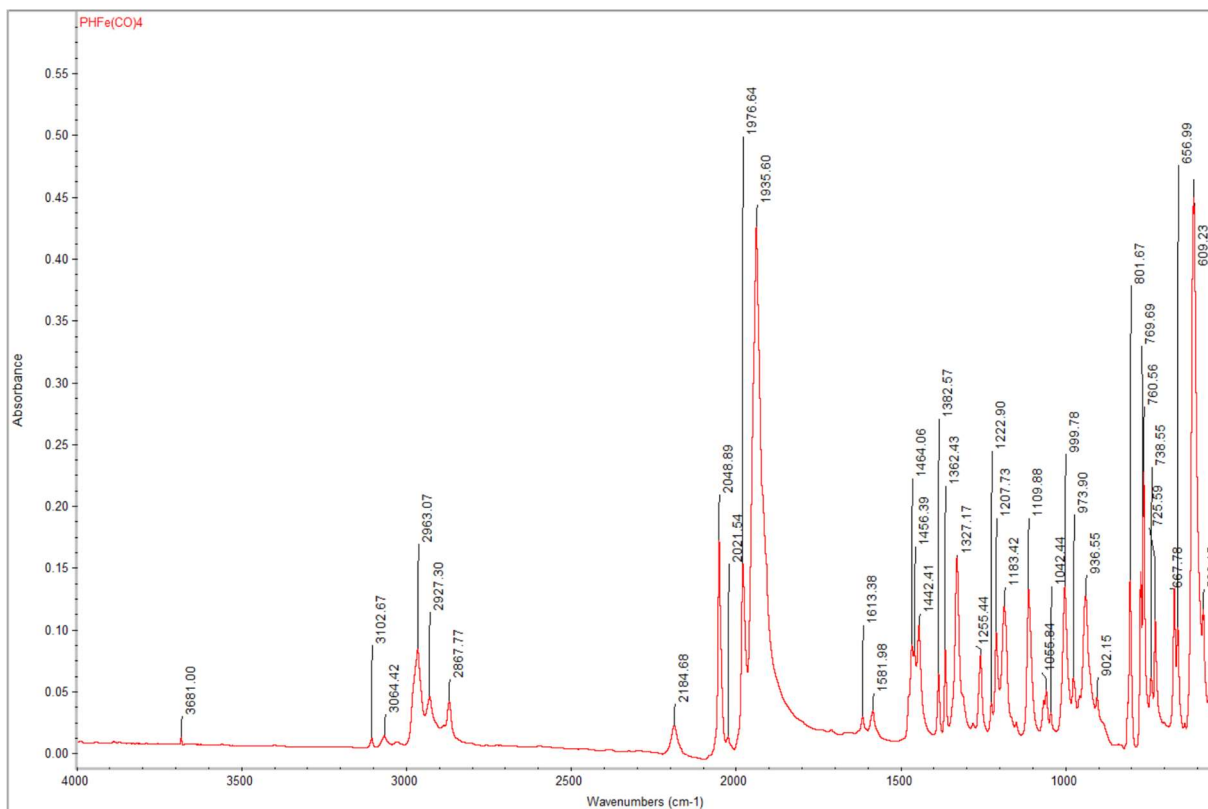


Figure S43. FTIR spectrum of 9.

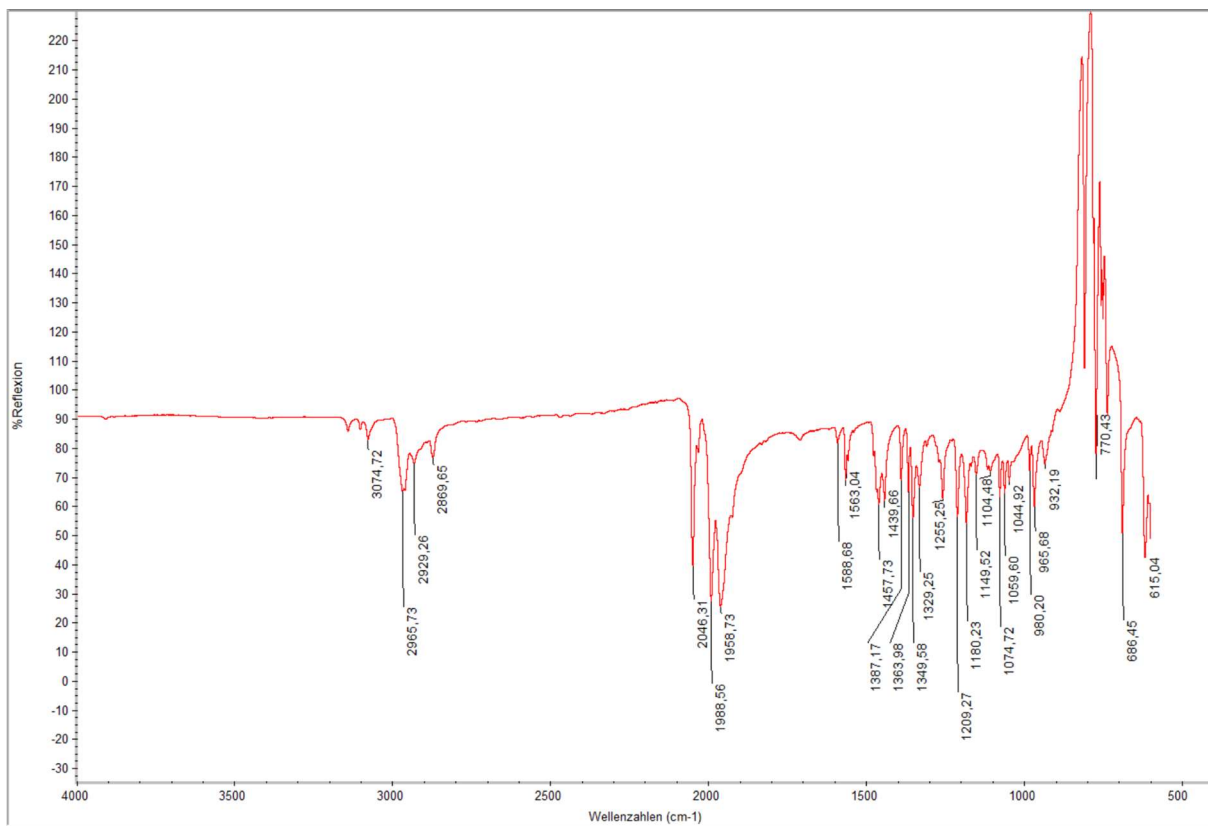


Figure S44. FTIR spectrum of 10c.

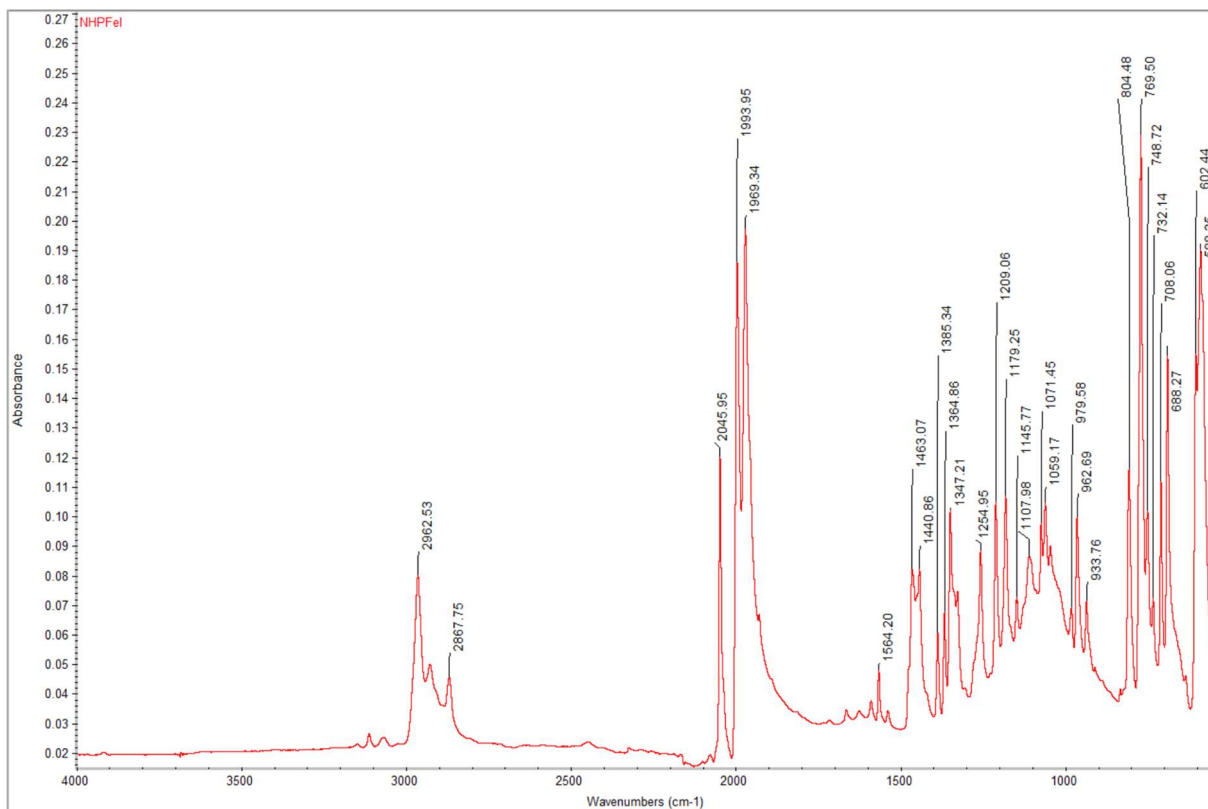


Figure S45. FTIR spectrum of **10d**.

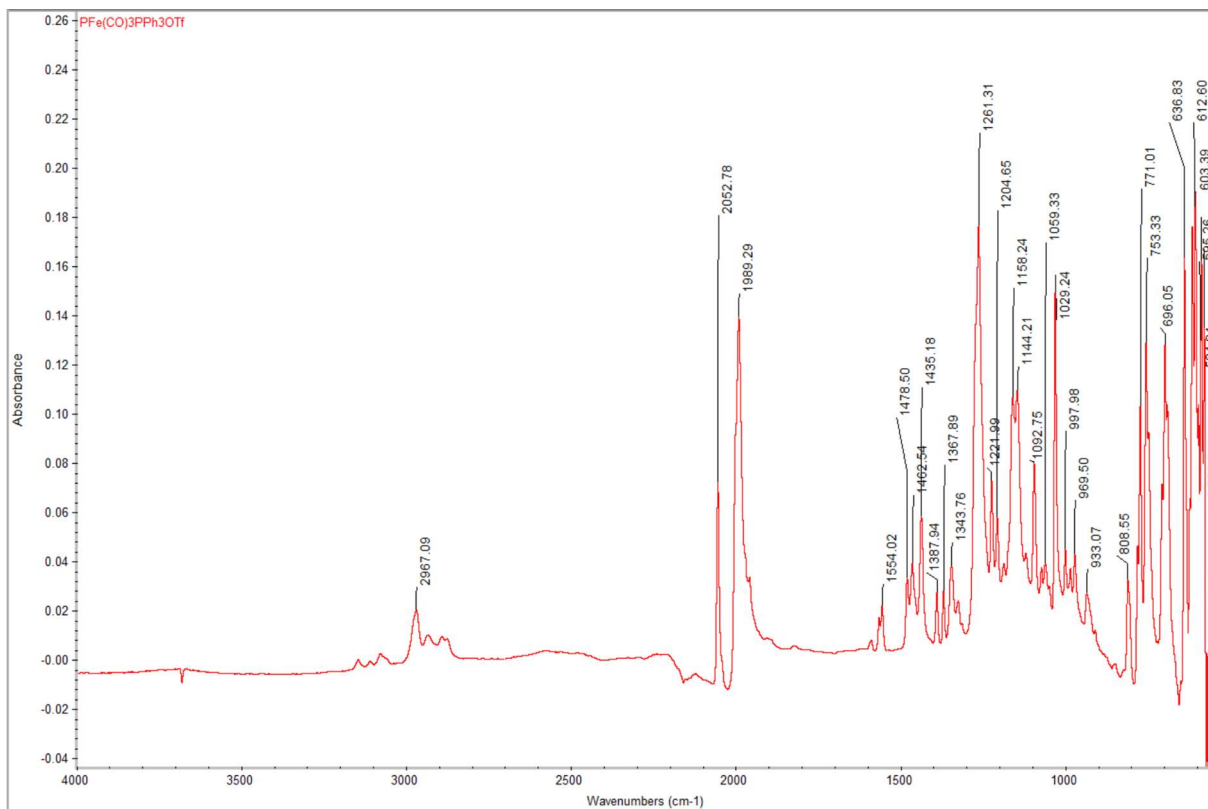


Figure S46. FTIR spectrum of **[15]OTf**.

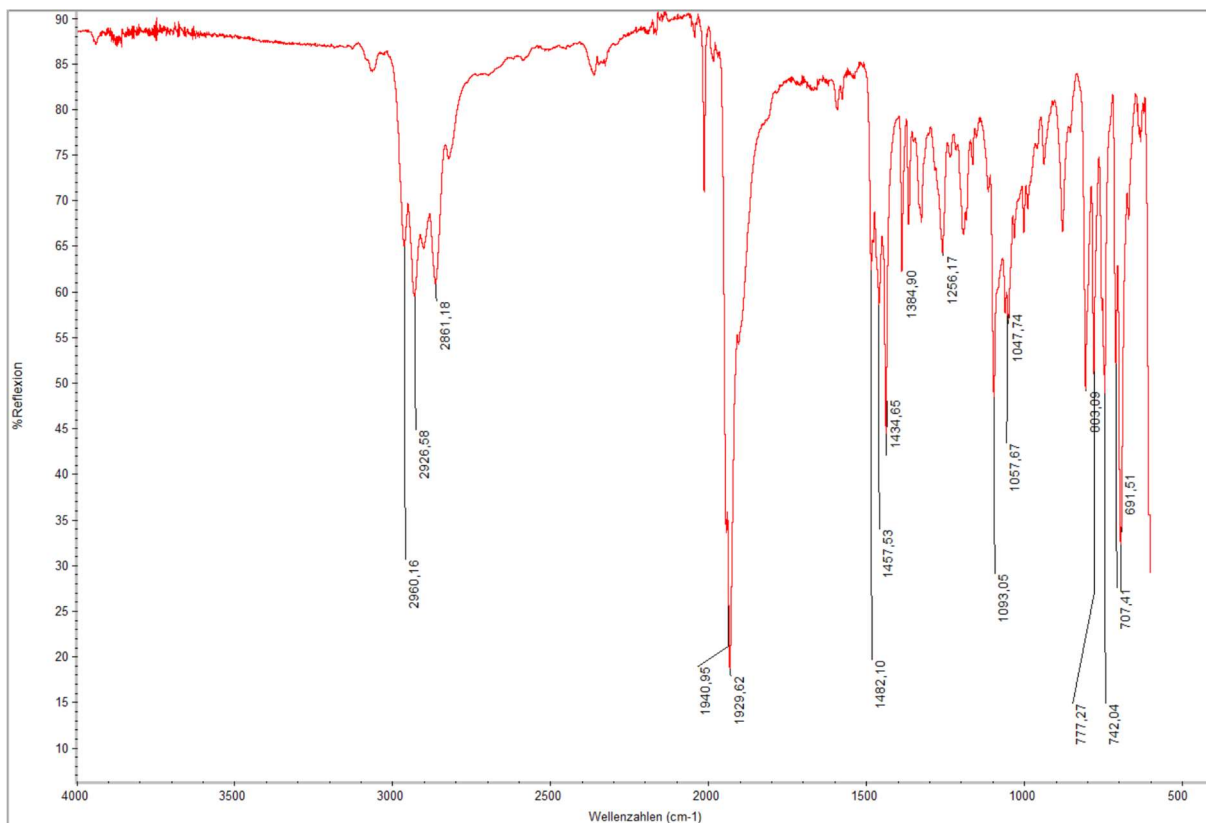


Figure S47. FTIR spectrum of crude 16.

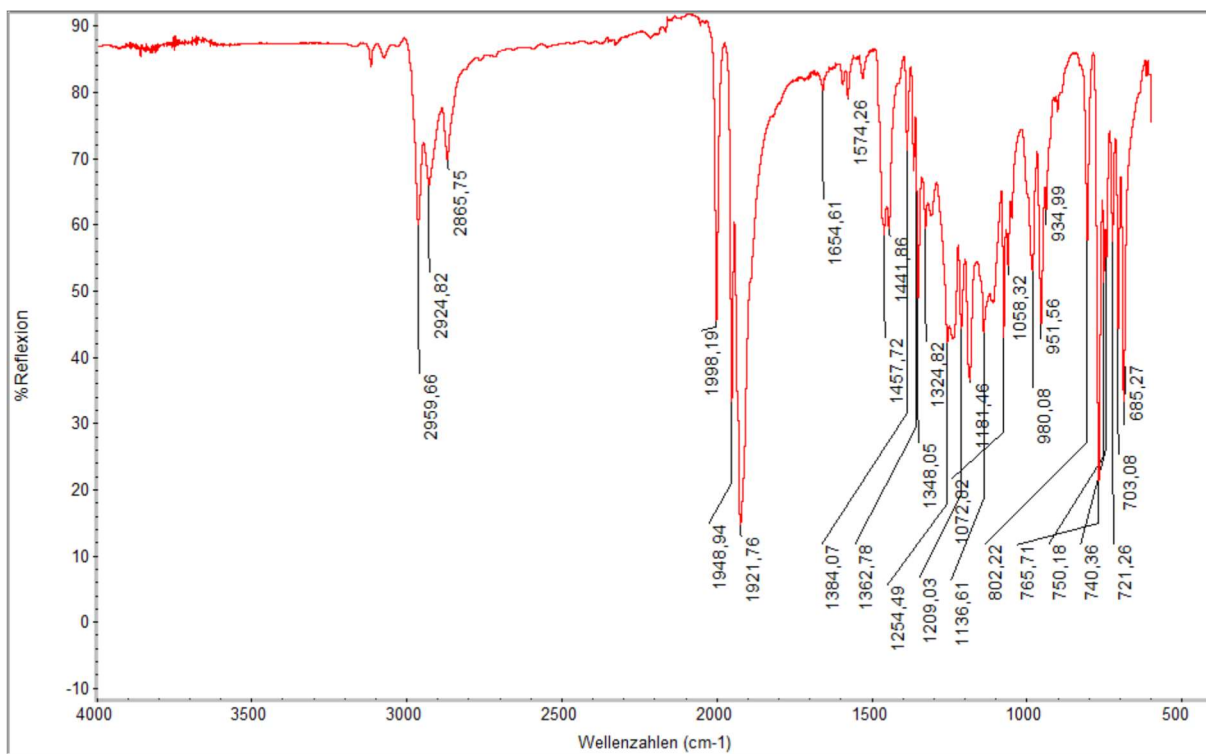
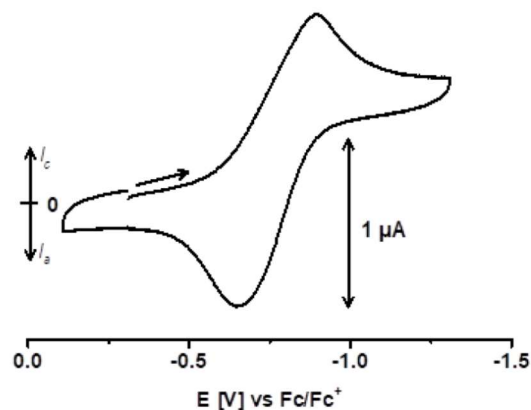


Figure S48. FTIR spectrum of (12)<sub>2</sub>.

## Electrochemistry and Spectro-electrochemistry

**General remarks.** Cyclic voltammetry studies were carried out using a EG&Princeton Applied Research M27A potentiostat equipped with a function generator M175. Measurements were carried out using a three electrode

setup consisting of Pt working and counter electrodes and Ag reference electrode in 0.1 M [Bu<sub>4</sub>N]OTf solution in THF. Potentials were referenced internally vs. Fc/Fc<sup>+</sup>. IR spectro-electrochemical measurements were carried out at -70 °C using a Thermo Scientific/Nicolet 6700 FTIR spectrometer equipped with a low-temperature OTTLE cell (optically transparent thin-layer electrochemical cell) and a cryostat.<sup>13,14</sup> Electrode potentials were controlled using a Metrohm Autolab B.V. PGSTAT101 potentiostat.



**Figure S49.** Cyclic voltammogram of a solution of [3]OTf in THF recorded at -78 °C (scan rate 100 mV/s, conducting salt [Bu<sub>4</sub>N]OTf,  $I_c/I_a = 0.96$ ).

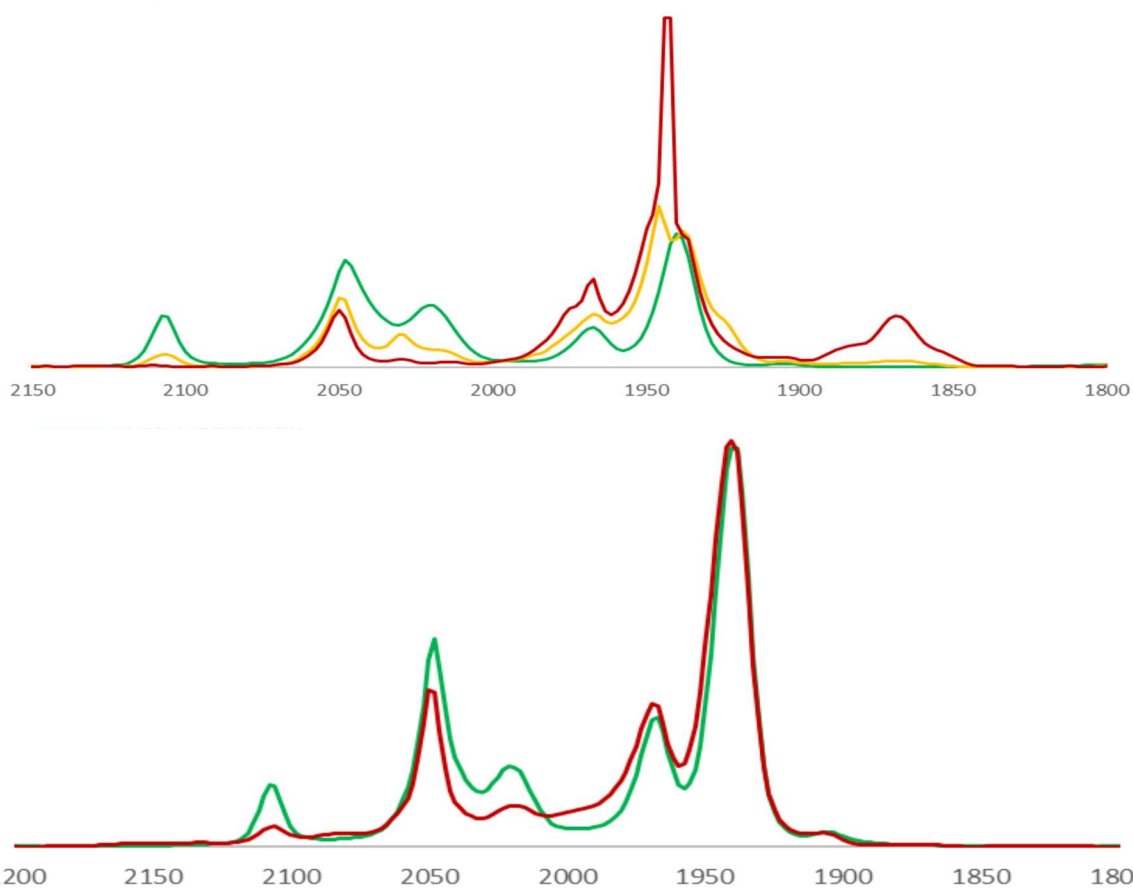


**Figure S50.** IR spectra recorded during a spectro-electrochemical study of the reduction of [3]OTf in THF at -70 °C. Top diagram: green trace - initial spectrum recorded prior to electrochemical reduction, yellow trace – intermediate spectrum, red trace – final spectrum. Bottom diagram: spectrum recorded after re-oxidation of the sample (red trace) with the initial spectrum (green trace) shown for comparison.

## Computational studies

**General remarks.** DFT calculations were carried out with the Turbomole<sup>15</sup> program package using the PBE functional<sup>16</sup> with Weigend's and Ahlrichs' def2-SVP and def2-TZVP basis sets<sup>17</sup> on an m4 grid for numerical integration. Grimme's D3BJ formalism<sup>18</sup> was applied to include dispersion effects and solvation was simulated using the COSMO-RS formalism<sup>19</sup> using the solvent parameters for THF. The molecular structures were established by full energy optimization at the COSMO-RS-RI-PBE-D3BJ/def2-SVP level. Numerical vibrational frequency calculations were carried out at the same level to identify the resulting stationary points as local minima (only positive normal modes) or transition states (one imaginary normal mode). Electronic energies were recalculated at the final geometries at the COSMO-RS-RI-PBE-D3BJ/def2-TZVP level. Standard Gibbs free energies  $\Delta G^0$  (for p=1 bar and T=298.13 K) of local minima and transition states were computed using these energies with the corrections obtained with the smaller basis sets. Relaxed potential energy scans (PES) were carried out at the COSMO-RS-RI-PBE-D3BJ/def2-SVP level, using the optimized structures as starting points. EPR parameters were calculated as recommended elsewhere<sup>20</sup> at the COSMO-RS-RI-PBE0/x2c-QZVPall-2c level using the optimised geometries. NBO population analyses were carried out using the modules implemented in the Turbomole package.

**Table S2.** Computed energies, chemical potentials  $\mu$  (all values in Hartree; atomic coordinates in .xyz format are contained in a separate file), and relative Gibbs free energies for molecules with even electron counts identified as local minima on the potential energy hypersurface.

Compound <sup>a)</sup>	$E_{dz}$ /Hartree <sup>b)</sup>	$\mu$ /Hartree <sup>b)</sup>	$E_{tz}$ /Hartree <sup>c)</sup>	$\Delta G^{0,rel}$ /kcal mol <sup>-1</sup> <sup>d)</sup>
[3] <sup>+</sup>	-3176.758324	0.510963	-3178.758097	--
8a <sub>eq</sub>	-3276.631764	0.511461	-3278.760103	2.2
8a <sub>ax</sub>	-3276.631103	0.509500	-3278.761605	0.0
8b <sub>eq</sub>	-3636.825445	0.510114	-3638.985040	0.0
8b <sub>ax</sub>	-3636.822071	0.508815	-3638.982605	0.7
8c <sub>eq</sub>	-5750.417261	0.508661	-5752.730153	0.0
8c <sub>ax</sub>	-5750.412719	0.505517	-5752.726484	0.3
8d <sub>eq</sub>	-3474.645651	0.507419	-3476.655439	0.0
8d <sub>ax</sub>	-3474.641779	0.507435	-3476.651185	2.8
9 <sub>eq</sub>	-3177.496829	0.517521	-3179.499856	5.8
9 <sub>ax</sub>	-3177.502756	0.515973	-3179.507630	0.0
CO	-113.103266	-0.014254	-113.237895	--
10a	-3163.452604	0.503202	-3165.447866	34.7 <sup>e)</sup>
10b	-3523.683703	0.502602	-3525.712348	8.2 <sup>e)</sup>
10c	-5637.282178	0.500031	-5639.464311	3.2 <sup>e)</sup>
10d	-3361.516955	0.500563	-3363.396575	-0.1 <sup>e)</sup>
11a	-3163.458575	0.504162	-3165.458395	26.5 <sup>e)</sup>
11b	-3523.654490	0.502749	-3525.686053	24.8 <sup>e)</sup>
4	-3064.362911	0.507708	-3066.235772	7.2 <sup>e)</sup>

a) ax end eq denote stereoisomers with the P-donor ligand in axial and equatorial position of the tpb coordination sphere of the Fe atom. b) at the COSMO-RS-RI-PBE-D3BJ/def2-SVP level of theory. c) at the COSMO-RS-RI-PBE-D3BJ/def2-TZVP//COSMO-RS-RI-PBE-D3BJ/def2-SVP level of theory. d)  $\Delta G^{0,rel} = E_{tz} + \mu$  relative to the most stable stereoisomer of **8a-d**, respectively. e) for **10a-d/11a,b/4** + CO

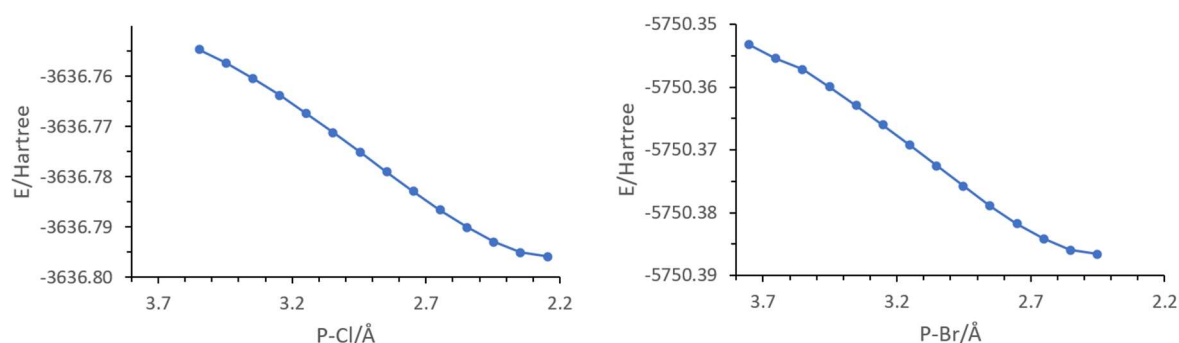


**Figure S51.** Results of relaxed potential energy scans showing the change in energy during the approach of a Cl<sup>-</sup> (left) and Br<sup>-</sup> ion (right) to the cation [3]<sup>+</sup> until the equilibrium distances are reached. Calculations were performed at the RI-PBE/def2-SVP level of theory.

**Table S3.** Computed energies and chemical potentials  $\mu$  (all values in Hartree; atomic coordinates in .xyz format are contained in a separate file) for transition states.

Compound	$E_{dz}$ /Hartree <sup>a)</sup>	$\mu$ /Hartree <sup>a)</sup>	$E_{tz}$ /Hartree <sup>b)</sup>	$\Delta G^{0,rel}$ /kcal mol <sup>-1</sup> <sup>c)</sup>
TS2 ( <b>8a</b> – <b>11a</b> )	-3276.553314	0.505605	-3278.686160	44.9
TS1 ( <b>8b</b> – <b>10b</b> )	-3636.755741	0.504312	-3638.918684	38.0
TS1 ( <b>8c</b> – <b>10c</b> )	-5750.350922	0.503826	-5752.667177	36.5
TS1 ( <b>8d</b> – <b>10d</b> )	-3474.585429	0.502936	-3476.599106	32.5
TS1 ( <b>9</b> – <b>4</b> )	-3177.423707	0.509206	-3179.431301	43.6

a) at the COSMO-RS-RI-PBE-D3BJ/def2-SVP level of theory. c) at the COSMO-RS-RI-PBE-D3BJ/def2-TZVP//COSMO-RS-RI-PBE-D3BJ/def2-SVP level of theory. c)  $\Delta G^{0,rel} = E_{tz} + \mu$  relative to the most stable stereoisomer of **8a-d**, respectively.

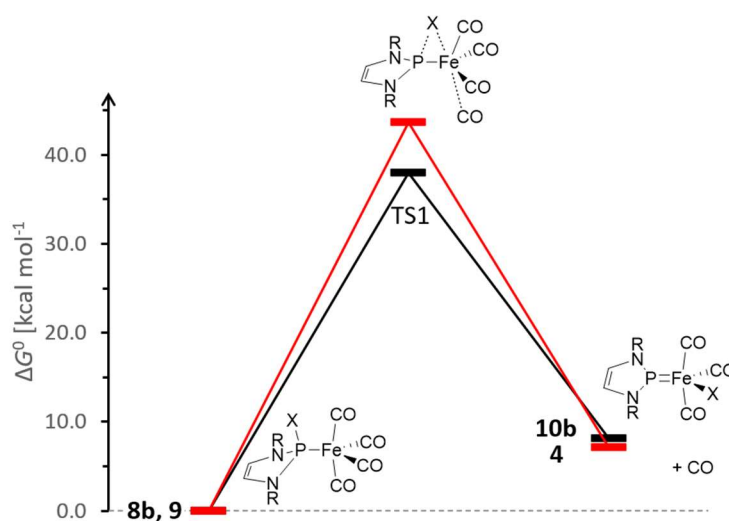


**Figure S52.** Minimum Gibbs free energy reaction pathways for the decarbonylation of **9** and **8b** (for comparison) calculated at the COSMO-RS-RI-PBE/def2-TZVP//COSMO-RS-RI-PBE/def2-SVP level of theory. The values of  $\Delta G^0$  refer to the stereoisomer with the P-donor ligand in axial (**9**) and equatorial (**8b**) position, respectively. Colour coding: black (**8b/10b**, X = Cl), red (**9/4**, X = H).

**Table S4.** Computed energies, isotropic  $g$ -values and hyperfine coupling constants  $A(^{31}\text{P})$  for radicals **3\*** and **13\***.

Compound	$E_{\text{COSMO-RS-RI-PBE-D3BJ/def2-SVP}}$	$\bar{E}_{\text{COSMO-RS-RI-PBE0-D3BJ/x2c-QZVPall-2c}}$	$g$	$A(^{31}\text{P})/\text{mT}$ <sup>a)</sup>
<b>3*</b>	-3176.909086	-3177.350875	2.0077	13.4
<b>12*</b>	-3063.753021	-3064.081915	2.0799	1.40

a) Values calculated in MHz were converted to mT using the formula  $A(\text{mT}) = A(\text{MHz})/(g \cdot 13.9962)$ .

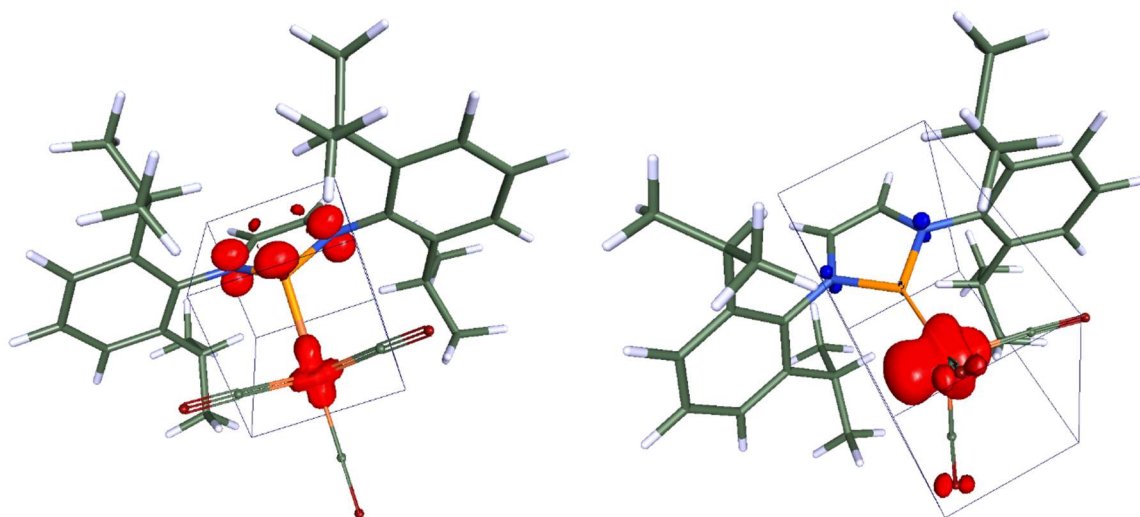


**Figure S53.** Graphical representation of the calculated spin density (COSMO-RS-RI-PBE0/x2c-QZVPall-2c//COSMO-RS-RI-PBE-D3BJ/def2-SVP level) for **3•** (left) and **12•** (right).

## References

- 1 S. Burck, D. Gudat, K. Nättinen, M. Nieger, M. Niemeyer and D. Schmid, *Eur. J. Inorg. Chem.*, **2007**, 5112.
- 2 S. Burck, D. Gudat, M. Nieger, W.W. du Mont, *J. Am. Chem. Soc.*, **2006**, *128*, 3946.
- 3 D. Herrmannsdörfer, M. Kaaz, O. Puntigam, J. Bender, M. Nieger, D. Gudat, *Eur. J. Inorg. Chem.*, **2015**, 4819.
- 4 J. A. S. Howell, B. F. G. Johnson, P. L. Josty, J. Lewis, *J. Organomet. Chem.* **1972**, *39*, 329.
- 5 V. Yu. Kukushkin, A. I. Moiseev, *Inorg. Chim. Acta*, **1990**, *176*, 79.
- 6 R. H. Harris, E. D. Becher, S. M. Cabral de Menezes, R. Goodfellow, P. Granger, *Concepts Magn. Reson.*, 2002, **14**, 326.
- 7 S. Stoll, A. Schweiger, *J. Magn. Reson.*, **2006**, *178*, 42.
- 8 T. Li, A. J. Lough, R. H. Morris, *Chem. Eur. J.*, **2007**, *13*, 3796.
- 9 G. M. Sheldrick, *Acta Cryst.* 2008, **A64**, 112.
- 10 G. M. Sheldrick, *Acta Crystallogr.*, **2015**, *A71*, 3.
- 11 G. M. Sheldrick, *Acta Crystallogr.*, **2015**, *C71*, 3.
- 12 S. Parson, H. D. Flack, T. Wagner, *Acta Crystallogr.*, **2013**, *B69*, 249.
- 13 F. Hartl, H. Luyten, H. A. Nieuwenhuis, G. C. Schoemaker, *Appl Spectrosc* **1994**, *48*, 1522.
- 14 T. Mahabiersing, H. Luyten, R. C. Nieuwendam, F. Hartl, *Collect. Czech. Chem. Commun.* **2003**, *68*, 1687.
- 15 a) S. G. Balasubramani; G. P. Chen; S. Coriani; M. Diedenhofen; M. S. Frank; Y. J. Franzke; F. Furche; R. Grotjahn; M. E. Harding; C. Hättig; A. Hellweg; B. Helmich-Paris; C. Holzer; U. Huniar; M. Kaupp; A. Marefat Khah; S. Karbalaei Khani; T. Müller; F. Mack; B. D. Nguyen; S. M. Parker; E. Perlt; D. Rappoport; K. Reiter; S. Roy; M. Rückert; G. Schmitz; M. Sierka; E. Tapavicza; D. P. Tew; C. van Wüllen; V. K. Voora; F. Weigend; A. Wodynski; J. M. Yu. Turbomole, *J. Chem. Phys.*, **2020**, *152*, 184107; b) TURBOMOLE V7.7 2022, a development of University of Karlsruhe and Forschungszentrum Karlsruhe GmbH, 1989-2007, TURBOMOLE GmbH, since 2007; available from <https://www.turbomole.org>.
- 16 J. P. Perdew; K. Burke; M. Ernzerhof, *Phys. Rev. Lett.*, **1996**, *77*, 3865.
- 17 F. Weigend, R. Ahlrichs, *Phys. Chem. Chem. Phys.* 2005, *7*, 3297.
- 18 S. Grimme, S. Ehrlich, L. Goerigk, *J. Comp. Chem.* 2011, **32**, 1456.
- 19 A. Klamt, V. Jonas, T. Bürger, J. C. W. Lohrenz, *Phys. Chem. A*, **1998**, *102*, 5074.
- 20 F. Bruder, Y. J. Franzke, F. Weigend, *J. Phys. Chem. A*, **2022**, *126*, 5050.